Surface modification strategies and the functional mechanisms of gold nanozyme in biosensing and bioassay

Sanam Garehbaghi [a], Amir M. Ashrafi [b], Vojtěch Adam [b], Lukáš Richtera [b,*]

[a] *Central European Institute of Technology, Brno University of Technology, Purkynova 123, Brno, CZ-612 00, Czech Republic*
[b] *Department of Chemistry and Biochemistry, Mendel University in Brno, Zemedelska 1, Brno, CZ-613 00, Czech Republic*

ARTICLE INFO

ABSTRACT

Gold nanozymes (GNZs) have been widely used in biosensing and bioassay due to their interesting catalytic activities that enable the substitution of natural enzyme. This review explains different catalytic activities of GNZs that can be achieved by applying different modifications to their surface. The role of Gold nanoparticles (GNPs) in mimicking oxidoreductase, helicase, phosphatase were introduced. Moreover, the effect of surface properties and modifications on each catalytic activity was thoroughly discussed. The application of GNZs in biosensing and bioassay was classified in five categories based on the combination of the enzyme like activities and enhancing/inhibition of the catalytic activities in presence of the target analyte/s that is realized by proper surface modification engineering. These categories include catalytic activity enhancer, reversible catalytic activity inhibitor, binding selectivity enhancer, agglomeration base, and multienzyme like activity, which are explained and exemplified in this review. It also gives examples of those modifications that enable the application of GNZs for *in vivo* biosensing and bioassays.

1. Introduction

Similar to a wide range of nanomaterials, gold based nanomaterials in the form of nanoparticle, nanocluster or single atom are considered as nanozymes (NZs) since they are endowed with innate catalytic activity like natural enzymes [1,2]. In fact, for the first time in 2004, Manea et al. used the term nanozyme for modified gold nanoparticles (GNPs) with transphosphorylation activity [3]. Gold nanozymes (GNZs) are mainly nanoparticles, which have intrinsic oxidoreductase activities such as peroxidase, oxidase, superoxide dismutase (SOD), catalase, and reductase [4]. GNPs also have partial role in mimicking other catalytic activities like helicase [5] and phosphatase [6]. NZs are preferred compared to natural analogues because of their lower production cost, higher recyclability, reusability and stability in a wider range of pH and temperature [7]. Particularly, GNZs are attracting a significant attention because of their multienzyme like activities, excellent stability, biocompatibility and feasible surface modification [8–10]. GNZs catalyze the substrate reaction by lowering the activation energy similar to a cofactor or metal complex in active site of natural enzymes with a metal ion catalysis mechanism. In a metal-ion catalysis, GNZs similar to multivalent metals, transfer electron/s to the substrate, or make conformational changes in substrate by hydrophobic binding [2,11].

Because of their inherent features GNZs are applied in clinical diagnosis, food safety, and environmental biosensing and bioassays by modulating its enzymatic activity. During detection process using GNZs, a substrate undergoes a catalytic reaction and generates an electrochemical, fluorescent, or colorimetric response [4]. The NZs entered in the biosensing field of study in 2007 [12], however the application of GNZs in biosensing was first reported by Jv et al. in 2010 where they used the peroxidase activity of cysteamine (cysa) modified GNZs for detection of H_2O_2 and glucose in a cascade system along with glucose oxidase [13].

The use of GNZs in biosensing and bioassays is limited due to their poor catalytic activity and substrate selectivity. Since the catalytic reaction occurs on the surface of GNZs, the surface modification has an important impact on modulating GNZs' biomimetic activity. Further, the surface modification of GNZs makes an interaction with target analyte which is the substrate itself or competes with the substrate to interact with the surface of GNZs [14]. Researchers suggested that the rational surface modification approach in application of GNZs in biosensing and bioassays can enhance the target recognition properties or confer them the target triggered catalytic activity to simulate/inhibit the catalytic activity [15].

Inspired from the catalysis mechanisms of natural enzymes, the surface of GNZs can be modified with functional groups, small molecules, or ions to play a synergistic role in enhancing a specific enzyme-like activity

List of abbreviations

AA	acrylic acid
AB	Agglomeration base
ABTS	2,2′-azino-bis(3-ethylbenzothiazoline-6-sulfonic acid)
AMPS	2-acrylamido-2-methyl-1-propanesulfonic acid
AOx	alcohol oxidase
APBA	aminophenylboronic acid
Arg	arginine
ATP	adenosine triphosphate
GNPs	gold nanoparticles
BSA	bovine serum albumin
BSE	Binding selectivity enhancer
BSPP	bis(p-sulfonatophenyl)phenylphosphane dehydrate dipotassium salt
E. coli	*escherichia coli* bacteria
CAE	catalytic activity enhancer
CB [7].	cucurbit [7]uril
CMF	carbon microfibre
CS	cascade system
CTAB	cetyltrimethylammonium bromide
cyclen	1,4,7,10-tetraazacyclododecane
DAP	2,3-diaminophenazine
DMAPMA	N-(3-(dimethylamino)propyl)methacrylamide
dsDNA	double stranded DNA
EGDMA	ethylene glycol dimethacrylate
FCC	face-centered cubic
GMP	guanosine triphosphate
GNCs	gold nanocluster form nanozymes
GNRs	gold nanorod shape nanozymes
GNZs	gold nanozymes
GO	graphene oxide
GOx	glucose oxidase
HCV	hepatitis C virus
HER2	human epidermal growth factor receptor 2
HHTP	2,3,6,7,10,11-hexahydroxytriphenylene
HIV	human immunodeficiency virus
HRP	horseraddish peroxidase
K_{cat}	turnover rate

K_M	Michaelis-Menten constant
leu	leucine
LP	liposome
MAA	methacrylic acid
MBA	N,N'-Methylenebisacrylamide
MIP	molecularly imprinted polymer
MOF	metal organic framework
$MSiO_2$	mesoporous silica
MWCNT	multiwall carbon nanotube
NADH	nicotinamide adenine dinucleotide
NIPAAm	N-isopropylacrylamide
NLISA	nanonzyme-linked immunosorbent assay
NS	nanosheet
OPD	o-phenylenediamine
P. aerug	*Pseudomonas aeruginosa* bacteria
PAMAM	poly(amidoamine)
PB	prussian blue
PEG	polyethylene glycol
PNIPAM	poly(N-isopropylacrylamide)
PVP	polyvinylpyrrolidone
QD	quantum dot
RCAI	reversible catalytic activity inhibitor
rGO	reduced graphene oxide
SA	sodium alginate
SOD	Superoxide dismutase
S. aureus	*Staphylococcus aureus* bacteria
SDZ	sulfadiazine
Ser	serine
SERS	surface-enhanced raman spectroscopy
TSAb	target analyte specific antibody
TSAg	specific antigen for target analyte specific antibody
TSAp	target analyte specific aptamer
TSp	target analyte specific peptide
ssDNA	single stranded DNA
ssRNA	single stranded RNA
TACN	1,4,7-triazacyclononane
TMB	3,3′,5,5′-tetramethylbenzidine
V_{max}	maximal reaction rate

[16]. Indeed, the metal atom in the active site of a natural enzyme is further coordinated with amino acids or ligands containing donor-/acceptor groups to enhance the catalytic activity. Moreover, these groups improve the kinetic of catalytic activity via stabilizing transition state by facilitating adsorption of substrate and transferring electron assisted by catalysis, nucleophilic, or electrophile mechanism. Additionally the H^+ or OH^- provide an acid-base mechanism of catalysis. These mechanisms of catalysis stabilize the transition state and lower the activation energy [11]. Additionally, unlike the natural enzymes, NZs including GNZs lack the substrate specific binding sites that results in their poor substrate selectivity. The binding site in natural enzymes consists of amino acid residues and spatial structures similar to substrate which can selectively bind to a substrate [16,17]. Moreover, applying modifications with affinity toward the substrate, on the surface of GNZs plays a role similar to binding pockets in active site of natural enzyme. These modifications include bioreceptors like antibody, synthetic antibody, and aptamers that enhance the selectivity of sensing by decreasing the chance of side reactions on the surface of GNZs [18,19]. Furthermore, using the modifications that suppress the catalytic activity of GNZs can enable a mechanism of detection where the catalytic activity is restored in the presence of target analyte [15]. Another type of modifications makes the GNZs less stable upon interaction with the target analyte that leads to the agglomeration which subsequently affect the catalytic activity of GNZs.

In a further sensing approach, the surface of the GNZs is subjected to different modifications to provide numerous enzyme activities existing simultaneously or interchangeably named as cascade system (CS) or logic gates (LG), respectively [9,15].

This review aims to summarize the application of GNZs in biosensing and bioassays that is categorized based on the type of the surface modification and functionality in sensing mechanism. This surface modifications for biosensing application are classified as catalytic activity enhancer (CAE), reversible catalytic activity inhibitor (RCAI), binding selectivity enhancer (BSE), agglomeration base (AB), and multienzyme like activity (MEA). These strategies are explained and exemplified in detecting various target analytes from vital/toxic molecules, ions, biomolecules, biomarkers, cancer cells, and pathogens for *in vivo* and *in vitro* applications.

2. Mechanism of catalytic activity

Similar to natural enzymes, the surface of GNPs can be used for the adsorption and activation of catalytic reactions [20]. This is related to the different enzymatic activities that can be provided by the GNZs because of their proficiency in donating/accepting electron to/from substrate, cleaving bond in substrate, and hydrophobic interaction with substrate while their crystallographic surfaces further have part in stabilizing the

transition state. GNPs can also have part in other enzyme like activities like helicase and phosphatase. In this section, three mechanisms of catalytic activities in presence of GNPs are discussed and exemplified.

2.1. Oxidoreductase

Oxidoreductase is a group of enzymes with catalytic activity that causes the oxidation or reduction of their substrates by accepting or donating electron to the substrate, which are as peroxidase, oxidase, catalase, SOD, and reductase [21]. In this process, GNZs adsorb the substrate to the surface stabilizing the transition state, so that the reaction of transferring substrate (transition analogue) to product becomes kinetically favorable. During the catalytic activity related to peroxidase, oxidase, catalase, SOD, Two covalently bonded oxygen atoms as in H_2O_2,

O_2, or $O_2^{\bullet-}$ molecules are adsorbed to Au atoms with one of three modes of adsorption, namely end-on, top-bridge-top, and bridge-bridge, on the surface of GNZs as presented in Fig. 1(a) [22]. Then GNZs transfer electron to the substrates [23]. However GNZs mostly have a crystallographic face-centered cubic (FCC) structure [24], where different facets provide different activation energies to the adsorption of two covalently bonded oxygen atoms [25]. Although the change of electron state in Au atom have a critical role in transferring electrons, further a crystallographic structure of the GNZs provides favorable kinetic for adsorption of H_2O_2, O_2, and $O_2^{\bullet-}$ molecules. The summary of the oxidoreductase activities is presented schematically in Fig. 1 (c) [26]. Four types of oxidoreductases were chosen for further discussion as follows based on their frequent application in biosensing and bioassays.
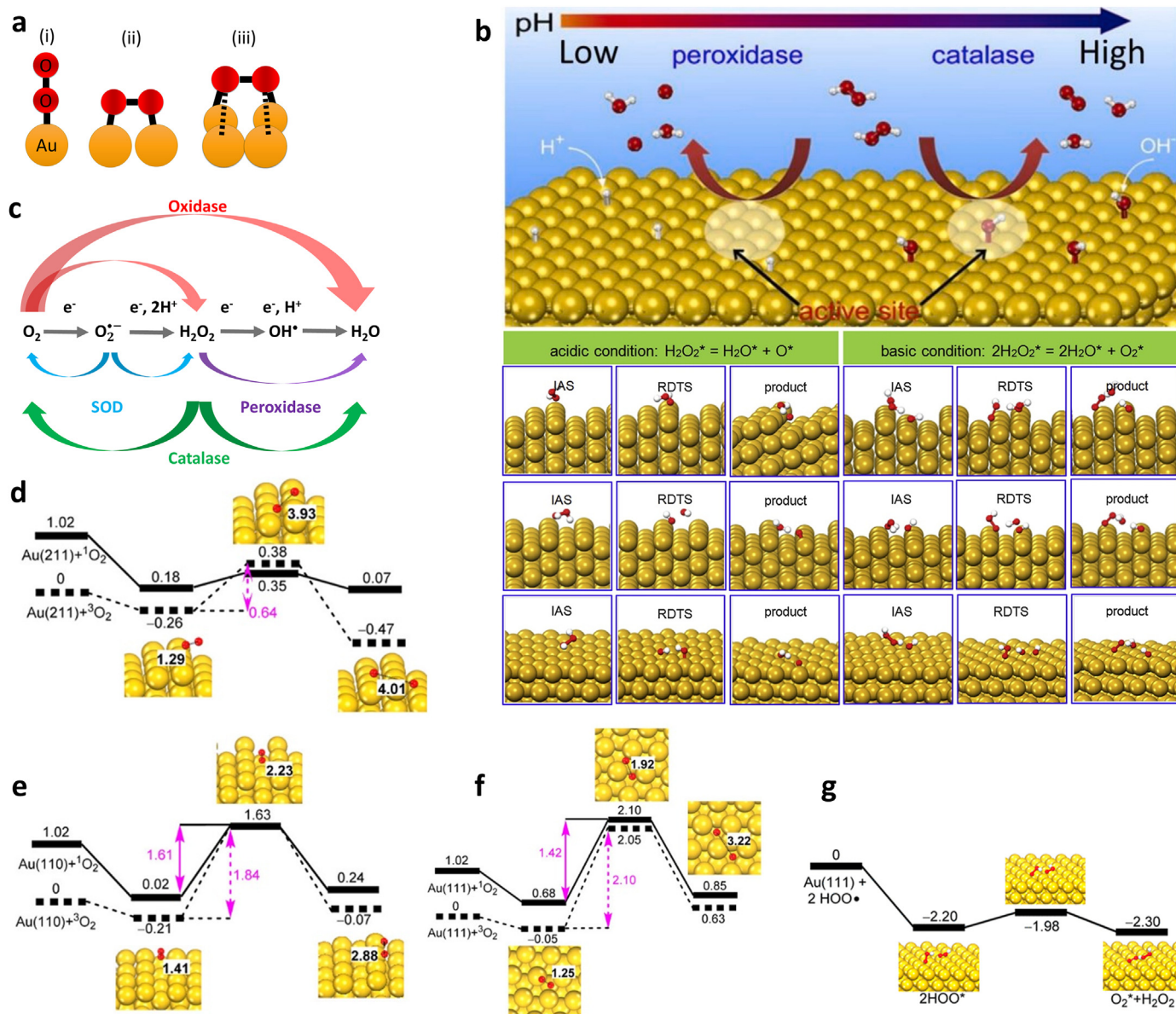
Fig. 1. Schematic diagrams to present: (a) adsorbing modes of O_2 on the surface of Au atoms as: (i) The end-on, (ii) top-bridge-top, (iii) and bridge-bridge, redrew from Ref. [22], with permission from The Royal Society of Chemistry, the copyright (2012), (b) peroxidase activity in acidic conditions (left) and catalase activity in basic conditions (right), reproduced from Ref. [27] with permission from the Elsevier, copyright (2015), both activities are described for Au(211) (top), Au(110) (middle) and Au(111) (bottom) in the bottom part of the figure, reproduced from Ref. [7] with permission from the Elsevier, copyright (2021), and (c) Review of the oxidoreductase activities, inspired from Ref. [26] The Royal Society of Chemistry, copyright (2019). (d) Oxidase activity for facet Au(211), (e) Oxidase activity for facet Au(110), (f) Oxidase activity for facet Au(111), (g) SOD activity for facet Au(111), reproduced from Ref. [25] with permission from the American Chemical Society, the copyright (2015), Note that in the figures d–g, the energies are measured in eV. These energies have been calculated by density functional theory, which has been in excellent agreement with experimental results.

2.1.1. Peroxidase

In the case of peroxidase enzymatic reactions, two substrates are used, where H_2O_2 as an acceptor substrate, oxidizes another donor substrate, and H_2O molecule is produced, as presented in Fig. 1(b-left) [27]. A peroxidase activity with two substrates can occur on the surface of GNZs with a ping-pong mechanism similar to natural enzyme. This type of reaction on GNZs conforms a similar ping-pong mechanism in two steps similar to natural enzymes [28]. In the first step, H_2O_2 as the first substrate is adsorbed on the surface of GNZs by the top-bridge-top mode. Then, it dissociates to hydroxide (OH^-) and hydroxyl ($OH^\bullet$) as products of transition state, later deprotonation of $OH^\bullet$, produces H_2O and an oxygen adatom stabilized on the surface of GNZ. The second substrate is oxidized by donating an electron to the oxygen adatom in the second step [25]. As an energetically favored facet for a peroxidase reaction, the (100) facet has the most stable transition state [22]. Another facet with peroxidase activity is the (211) [29]. For this type of reaction, an acidic environment is needed which protonate the surface of GNZs, with Bronsted-Lowry protons and enhance the transition state stability. GNZs can show peroxidase activity also similar to Fenton mechanism, in which the Au^{III} converts to Au^0 when H_2O_2 is decomposed to H^+ and $HO^\bullet_2$. In the second part of catalytic cycle Au^0 converts to Au^{III} when H_2O_2 is decomposed to $OH^\bullet$ and OH^- [30].

2.1.2. Oxidase

In an oxidase enzymatic reaction, dioxygen is used as an electron acceptor, where it is adsorbed on two gold atoms by the top-bridge-top mode [31]. In this reaction, Au atoms transfer electrons to the adsorbed oxygen molecules, to stabilize the transition state consisting of two adatoms. The oxygen adatom attacks the second substrate removing hydrogen bond in substrate. For the oxidase reaction, the least activation energy occurs on the (211) facet (Fig. 1(d)), while the highest activation energy is observed on (110) (Fig. 1(e)) and (111) facets (Fig. 1(f)) [25].

Different hydrocarbons can be oxidized with GNZs such as amines, alcohols, phenols, carbonyls, benzyls, and sugars, etc. where the product can be either H_2O or H_2O_2 molecule. One example is the glucose oxidation, when hydrated glucose anions interact with the gold atoms in GNZs, the interaction produces electron rich gold atoms, which in turn attack the molecular oxygen forming $Au^{I/II}$-O^{2-} intermediate. This intermediate helps to transfer electrons from glucose to the molecular oxygen producing H_2O_2 [22,32]. Another example is nicotinamide adenine dinucleotide (NADH) oxidation which is a coenzyme located inside cells. Since it is carrier of protons and electrons, it has hydrogen donor property. GNZs show the oxidase activity towards NADH, where first GNZs' coordinate with nitrogen atom in NADH, that results in adsorption of NADH on GNZs' surface and producing Au–H complex and NAD$^+$ as products. This is followed by removing of hydride from the surface of GNZs by the O_2 molecule to generate either H_2O or H_2O_2 [33].

2.1.3. Catalase

In this reaction H_2O_2 as the only substrate is adsorbed on the surface of Au atom by an end-on mode. The nucleophilic OH^- groups attack substrate and deprotonate it to produce $HO^\bullet_2$ and H^+ as products. Later as a second part of reaction, the formed Au-$HO^{\bullet-}_2$ intermediate reacts with another H_2O molecule and Au transfers electrons to $HO^{\bullet-}_2$ and produces O_2 and H_2O to complete the catalytic cycle. [15,34], as presented in Fig. 1(b-right) [35]. GNZs shows catalase activity at neutral to alkaline pH, in which the surface of Au atoms is hydrated by OH^- groups as Bronsted-Lowry base that stabilizes the transition state.

2.1.4. Superoxide dismutase (SOD)

SOD is an enzyme which scavenge superoxide radicals inside cell [36, 37]. GNZs with SOD like activity adsorb $O^{\bullet-}_2$ with an end-on mode with less activation energy on the surface, protonates this radical and produces $HO^\bullet_2$. The rearrangement of two Au-$HO^\bullet_2$ (Fig. 1(g)), forms H_2O_2 and O_2 [38] as end products of catalytic reaction. A study shows that

adsorption energy of GNZs increases for transition state in the order of Au^{III}-$O^\bullet_2$-Au^{III}, Au^{III}-$HO^\bullet_2$, Au^{III}–OH, Au^{III}–H. This leads to losing oxygen properties of GNZs from a range of peroxide to hydride in which makes GNZs more notable than other metal nanozymes [4,39].

2.1.5. Reductase

GNZs further possess reductase activity towards substrates like *p*-nitrophenol [40]. This activity is induced by sodium borohydride, and produces *p*-aminophenol and changes the color from yellow to colorless [41]. As it is presented in Fig. 2(a), in this reaction *p*-nitrophenol is adsorbed on the surface of GNZs and H atom produced from decomposition of $NaBH_4$ is adsorbed on GNZs and at the same time the reaction of H atom and *p*-nitrophenol produces *p*-aminophenol [42].

2.2. Helicase

Positively charged GNPs with L-cysteine (cys) modification can unzip a dsDNA similar to helicase enzyme, where GNPs bind double stranded DNA (dsDNA) from negatively charged phosphate backbone, weakening hydrogen bond between base pairs, and unzipping the dsDNA. This is carried out by pulling single stranded DNA (ssDNA) around clusters of GNZs making conformational changes and generating two ssDNAs, as presented in Fig. 2(b) [5,43]. However, to complete a helicase reaction GNPs should detach from ssDNA. Another study shows GNPs has less affinity towards ssDNA/RNA than dsDNA-RNA [44].

2.3. Phosphatase

Phosphatase-like activity is categorized in phosphomonoesterase and phosphodiesterase [45]. Modification of GNPs with organic-ions complex compounds like 1,4,7,10-tetraazacyclododecane (cyclen), and 1,4, 7-triazacyclononane (TACN) provides phosphomonoesterase-like activity, where this modification hydrolyses organic phosphates, by cleaving phosphomonoester bond (Fig. 2(c)). In this catalytic reaction, GNPs play two roles: first, making a hydrophobic interaction with substrate and second, improving the speed of H_2O dissociation that increases the generation of nucleophilic OH^- and H^+ [46]. Furthermore, modified GNPs also show phosphodiesterase activity and can cleave phosphodiester bond in RNA. For instance, the dioctylamine has two chiral thiolated heads that can be complexed with two zinc ions on the surface of GNPs. This modification can selectively cleave the uracil dinucleotide as demonstrated in Fig. 2(d) [47].

3. Surface modification of GNZs for *in vitro* biosensing mechanisms

In this section, five types of biosensing strategies with GNZs due to the modifications are discussed with related examples provided from the literature. Examples describe how interaction of modifying layer and target analyte is considered as a sensing strategy and give information about those biosensing platform properties that improve such as selectivity, sensitivity, linear dynamic range and limit of detection (LOD). One or a combination of these strategies can be applied in biosensors and bioassays according to requirements of detection. More examples are provided in Table 1.

3.1. Catalytic activity enhancer (CAE)

Modifying the surface of GNZs with ligands or biomolecules containing nucleophilic, electrophilic functional groups or multivalent elements can enhance the catalytic activity [48]. This is because of stabilizing the transition state via catalysis mechanisms of acid-base, electrophilic, or nucleophilic, that catalyzes the conversion of the substrate to the final products while transferring electron between GNZs and the substrate/s [11].
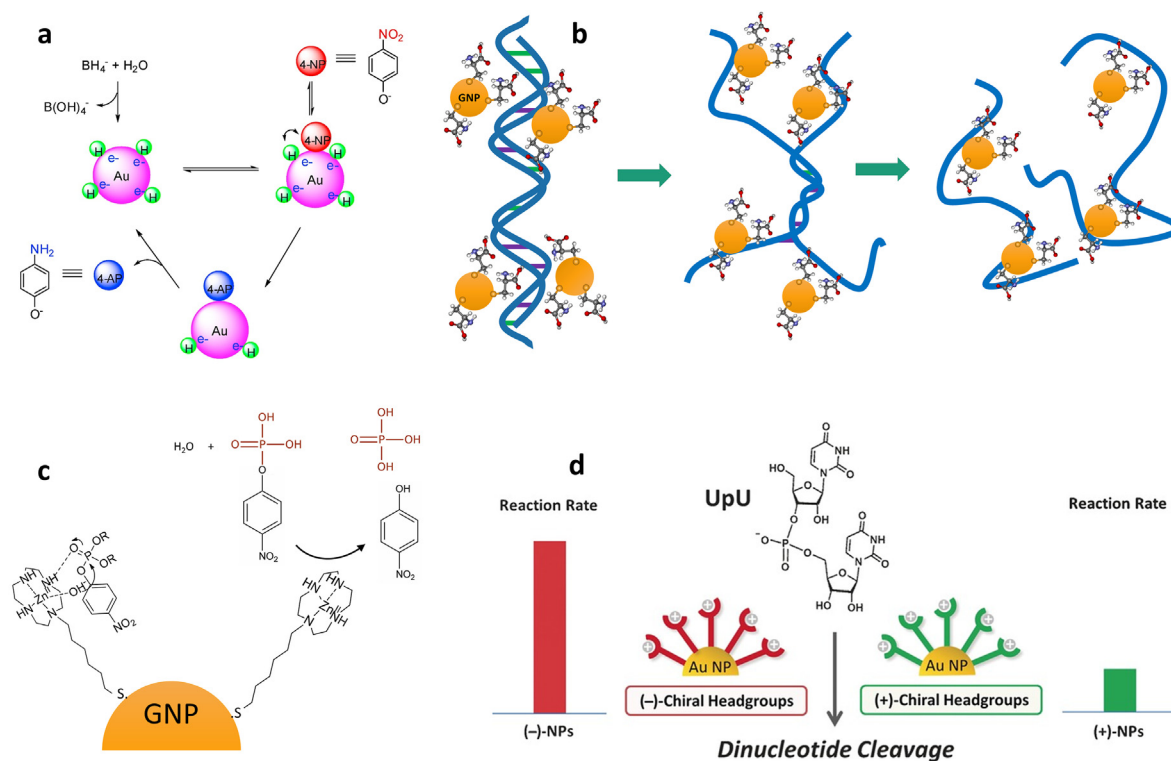
Fig. 2. Schematic diagram to present participation of GNPs in mimicking (a) reductase-like activity [42], reproduced with permission from the Elsevier, copyright (2015), (b) DNA helicase like activity, redrew from Ref. [5], with permission from the American Chemical Society, copyright (2016), (c) phosphatase-like activity, redrew from Ref. [46], with permission from the Elsevier, copyright (2021), (d) and phosphodiesterase like activity, reproduced from Ref. [47], with permission from John Wiley & Sons, the copyright (2016).

Table 1
List of Surface modifications and subsequent application of GNZs in biosensing and bioassays.

Modification	Mechanism	Catalytic Activity	Target Molecule	Linear Range	LOD	Technique	Ref
CMF-hemin GOx	CAE, CS	Peroxidase	Glucose	0.1–0.9 mM	0.05 mM	Amperometry	[95]
CMF-hemin AOx	CAE, CS	Peroxidase	Ethanol	0.01–0.15 mM	0.005 mM	Amperometry	[95]
Hemin-MOF-TSAb	CAE	Peroxidase	α-fetoprotein	0.080–43 ng/mL	0.020 ng/mL	Colorimetry	[96]
Cu-HHTP-MOF NS	CAE	Peroxidase	H_2O_2	50 nM–16.4 mM	5.6 nM	Amperometry	[97]
Pt@MSiO$_2$-TSAg	CAE	Peroxidase	Mumps virus	0.01–100 µg/mL	10 ng/mL	Colorimetry	[98]
MSiO$_2$	–	Peroxidase, Oxidase	*E. coli, S. aureus*	–	–	Colorimetry	[99]
PNIPAm	CS	Oxidase, Peroxidase	Glucose	10–70 mM	5.07 mM	Colorimetry	[100]
PNIPAm		Peroxidase	H_2O_2	3–15 mM	2.43 mM	Colorimetry	[100]
MoS$_2$-QDs	CAE	Peroxidase	Glucose	1–400 µM	0.068 µM	Colorimetry	[101]
DNA hydrogel-Ag$^+$	CS	Peroxidase	Glucose	5–100 µM	1.7 µM	Fluorescence	[102]
Zn^{II}-TACN complexe	CAE	Phosphotase	pBR322 plasmid	–	–	Agrose gel electrophoresis	[103]
Thiolated T10	CAE	Peroxidase	Hg^{2+}	50–2000 nM	10 nM	Colorimetry	[104]
GO	CAE	Peroxidase	H_2O_2	10 nM–10 mM	1.9 nM	Voltammetry	[105]
GO	CAE	Peroxidase	H_2O_2	0.01–5 mM	2µ M	Colorimetry	[105]
Tyrosine-TSAp	RCAI	Peroxidase	Norovirus	20–3300 virus/mL	30 virus/mL	Colorimetry	[57]
Citrate-TSAp	RCAI	Peroxidase	Zearalenone	10–250 ng/mL	10 ng/mL	Colorimetry	[106]
Citrate-TSAp	RCAI	Catalase	Pb^{2+}	0.13–53.33 nM	0.07 nM	SERS	[107]
Citrate-TSAp	RCAI	Peroxidase	*P. aerug*	–	60 CFU/mL	Amperometry	[108]
Tyrosine-TSAp	RCAI	Peroxidase	Kanamycin	0.1–60 nM	0.06 nM	Voltammetry	[109]
TSAp	RCAI	Peroxidase	Kanamycin	5–100 nM	2.28 nM	Colorimetry	[109]
Cysa	AB	Peroxidase	Choline	–	–	Colorimetry	[110]
CTAB-CeO$_2$	CAE	Peroxidase	Glucose	0.1–1 mM	–	Colorimetry	[111]
CTAB-CeO$_2$	LG	Catalase, peroxidase, SOD	–	–	–	–	[111]
CTAB-CeO$_2$	CAE	Peroxidase	Glucose	0.1–1 mM	–	Colorimetry	[111]

Table 1 (*continued*)

Modification	Mechanism	Catalytic Activity	Target Molecule	Linear Range	LOD	Technique	Ref
CTAB-CeO$_2$	LG	Catalase, peroxidase, SOD	–	–	–	–	[111]
Au–Pt, APBA monomer, MBA crosslinker	BSE	Oxidase	–	–	–	Colorimetry	[79]
DMAPMA or AMPS monomer	BSE	Peroxidase	TMB	–	–	Colorimetry	[112]
AA and NIPAAm monomer, MBA crosslinker	CAE	Peroxidase	ABTS	–	–	Colorimetry	[112]
Pt–SiO$_2$, MAA monomer, EGDMA crosslinker	BSE	Peroxidase	Sulfadiazine	–	–	Colorimetry	[80]
Graphene-TSAp	RCAI	Peroxidase	Hepatits C Virus	–	–	Colorimetry	[113]
Graphene-TSAp	RCAI	Peroxidase	Insuline	–	–	Colorimetry	[113]
Cysa	CAE	Oxidase	Glucose	18–1100 μM	4 μM	Colorimetry	[13]
Cysa	CAE	Peroxidase	H$_2$O$_2$	2.0–200 μM	0.5 μM	Colorimetry	[13]
Ag-hemin-rGO	CAE	Peroxidase	H$_2$O$_2$	10–35 nM	1.26 nM	Colorimetry	[114]
Ag-hemin-rGO	CAE	Peroxidase	Glucose	2–5 μM	425 nM	Colorimetry	[114]
Pt–SiO$_2$	CAE	Catalase	H$_2$O$_2$	0.1 pM–1 mM, 1 mM–10 M	0.1 pM	Colorimetry	[115]
MIL-101 MOF- lactate oxidase	CS	Peroxidase	Lactic acid	10–200 μM	5.0 μM	SER	[116]
MIL-101 MOF-GOx	CS	Peroxidase	Glucose	10–200 μM	4.2 μM	SER	[116]
Histidine	CAE	Peroxidase	Cu^{2+}	1–100 nM	0.1 nM	Colorimetry	[117]
Histidine-Cu^{2+}	RCAI	Peroxidase	Histidine	0.02–2.0 μM	20 nM	Colorimetry	[117]
Citrate	RCAI	Peroxidase	Hg^{2+}	0.1–200 μg/mL	1.2 ng/mL	Colorimetry	[112]
BSA	CAE	Peroxidase	Ag$^+$	0.5–10 μM	0.204 μM	Colorimetry	[118]
Fe-MIL-88 MOF-TSAp	RCAI	Peroxidase	HIV virus	30–150 nM	1.4 nM	Colorimetry	[119]
Citrate- TSAp	RCAI	Peroxidase	Thrombin	1–100 nM	0.1 nM	Colorimetry	[120]
ssDNA (A15, C15, and T15)	LG	Peroxidase	BSA, HRP	10–1000 nM 10–200 nM	10 nM	Colorimetry	[121]
TSAp	RCAI	Peroxidase	Abrin	0.2–17.5 nM	0.05 nM	Colorimetry	[122]
Graphene, TSAp	RCAI	Peroxidase	Hg^{2+}	0.01–0.5 μM	3.63 nM	Colorimetry	[123]
Graphene, TSAp	RCAI	Peroxidase	Microcystine LR	0.01–1.0 ng/mL	7.14 pg/mL	Colorimetry	[123]
Cysa, TSp	CAE	Peroxidase	Integrin GPIIb/IIIa	31.25–375 ng/mL	–	Colorimetry	[124]
Fe$_2$O$_3$ nanocube, IgG	CAE	Peroxidase	p53-specific autoantibody	–	0.12 U/mL	Colorimetry	[125]
Fe$_2$O$_3$ nanocube, IgG	CAE	Peroxidase	p53-specific autoantibody	–	0.08 U/mL	Amperometry	[125]
Heparin	AB	Peroxidase	Heparinase	0.1–3 μg/mL	0.06 μg/mL	Colorimetry	[126]
PEG-Fe$_3$O$_4$, PEG-folic acid	CAE	Peroxidase	HeLa cell	–	–	Colorimetry	[127]
GO-SiO$_2$-folic acid	CAE	Peroxidase	HeLa cell	250–500,000 cell/mL	250 cell/mL	Colorimetry	[128]
BSA-GNCs-LPs-TSAb	RCAI	Peroxidase	HER2	6–1000 cell/mL	6 cell/mL	Colorimetry	[129]
TSAb	CAE	Peroxidase	Avian influenza virus	10 pg/mL– 10 μg/mL	1.11 pg/mL	Colorimetry	[77]
TSAb-Ag shell	CAE	Peroxidase	Norovirus (NS14)	0.001–100 ng/mL	10.8 pg/mL	Colorimetry	[130]
CTAB, TSAp	AB	Peroxidase	Malachite green	10–500 nM	1.8 nM	Colorimetry	[131]
citrate-casein	RCAI	Peroxidase	Protease	1–0.1 ng/mL	44 ng/mL	Colorimetry	[132]

Modification of GNZs with biomolecules can enhance catalytic activity. For example, the peroxidase-like activity of GNZs towards glutathione is proved to be enhanced by immobilizing two amino acid residues as active sites on the surface. Selenocysteine is the active site of natural glutathione peroxidase which adsorbs H$_2$O$_2$. To this end, a synthetic pentapeptide Ser-Arg-Gly-Asp-Cys with SH bonding is self-assembled on the GNZs' surface so that selenium as an active site makes a bonding with the thiol head of glutathione. Fig. 3(a) presents the active site of this modification. A second active site of cysa, was further self-assembled on GNZ to absorb anionic substrate on its amine group. Taking advantage of the two active sites, this structure increases the peroxidase activity on GNZs by 14 times compared to the unmodified GNZs [28]. GNZs in the form of clusters (GNCs) can obtain peroxidase activity upon hybridization with lysozyme. The peroxidase activity is then enhanced by modifying the surface of graphene oxide with as prepared GNZs-lysozyme by electrostatic absorption and later incubation with folic acid. This method can be used to detect cancer cells, because these cells have folate receptors, which helps the cell to absorb the GNZs that enables them to oxidize TMB to generate an analytical signal proportional to the number cancer cells [49]. Apoferritin with hallow structure is composed of six amino acids that contain histidine. Histidine helps to adsorb gold and silver ions inside the cavity of the apoferritin forming Au–Ag-histidine nanozymes. This modification leads to increase the superoxidase and catalase activity of GNZs, because superoxide dismutase enzyme has histidine as the active site, which makes covalent coordination bonding with metallic cofactor, that helps to convert negative charge of protein to positive, and consequently to adsorb superoxide molecule, an example is presented in Fig. 3(b) [50]. When the GNCs-Pt alloy is modified with the guanosine monophosphate (GMP) it has peroxidase activity towards *o*-phenylenediamine (OPD). The products of this reaction include 2, 3-diaminophenazine (DAP) with a yellow color. The process of production is presented in Fig. 3(c) [51]. During oxidation of glucose with GOx enzyme, H$_2$O$_2$ molecule is produced. Detection of produced H$_2$O$_2$ can be performed by peroxidase activity of GNZs-GMP towards DAP. This colorimetry technique for detection of glucose has a wide linear range of 0.05–0.4 mM and low LOD of 11 μM.

Another form of enhancing the catalytic activity of GNZs is realized when the COOH, or NH$_2$ on the applied modification interact with the substrate by providing nucleophilic, electrophilic or acid-base catalysis. GNCs in general provide catalase-like activity at alkaline conditions, even
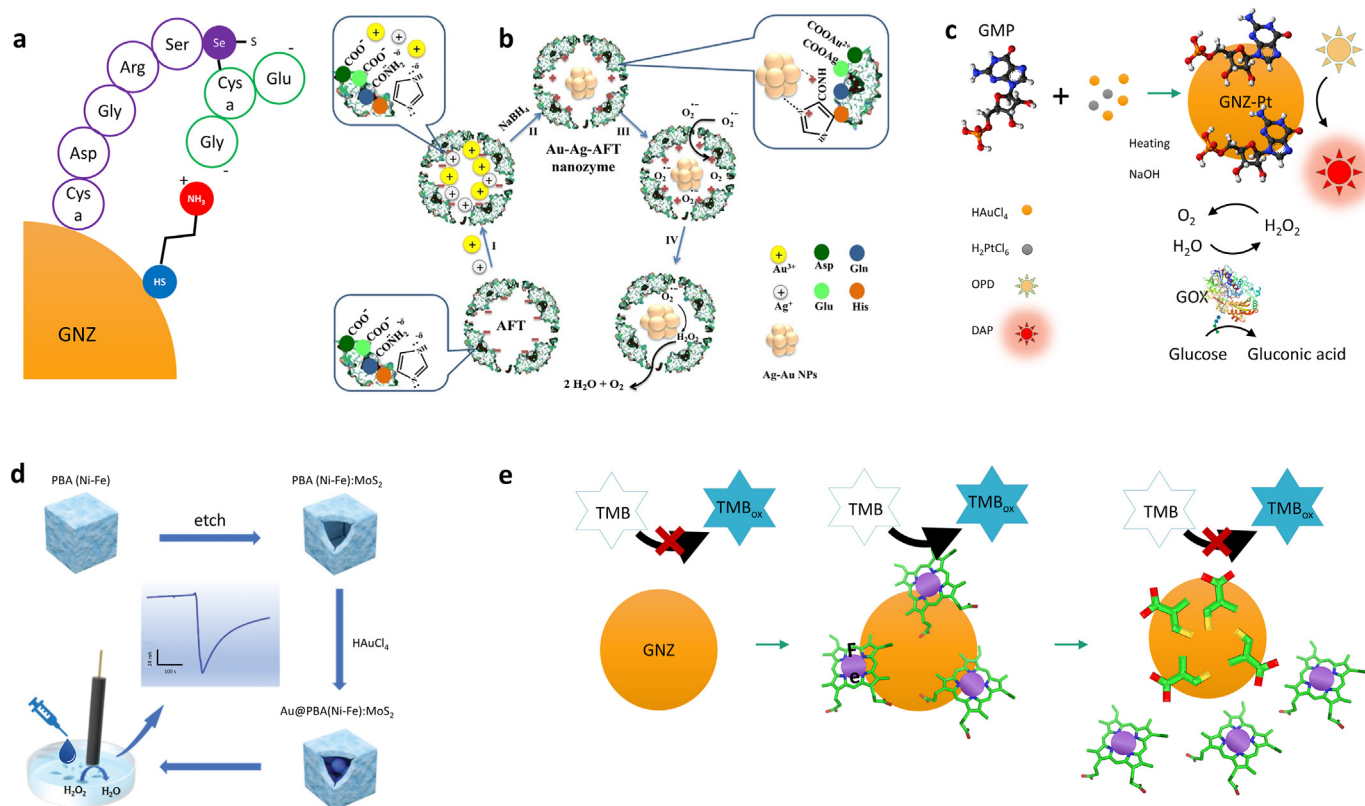
Fig. 3. Schematic diagrams with the CAE sensing mechanism: (a) in GNZs modified with two active sites and its interaction with glutathione, redrew from Ref. [28] with permission from The Royal Society of Chemistry, copyright (2020), (b) to present the synthesis of GNZs-silver-histidine, where functional groups in histidine act as active site with superoxidase activity, reproduced from Ref. [50] with permission from the Elsevier, copyright (2018), (c) GNZs-Pt-GMP modification and its peroxidase activity towards DAP, redrew from Ref. [51] with permission from the Elsevier, copyright (2022), (d) The production of GNZs with Prussian blue modification, reproduced and modified from Ref. [58], with permission from The Royal Society of Chemistry, copyright (2019), and (e) process of detecting cys by the GNZs-heme modification, reproduced from Ref. [64], with permission from The Royal Society of Chemistry, copyright (2021). (For interpretation of the references to color in this figure legend, the reader is referred to the Web version of this article.)

when they are modified with Polyvinylpyrrolidone (PVP) polymers. But, when the GNCs are modified with PAMAM (poly(amidoamine)) polymers, two types of modification can be obtained: The first is when the termination group of PAMAM is OH or COOH, the results show less catalase activity. The second is when termination group is NH_2, where the modification leads to increase the catalase-like activity at neutral and acidic conditions, and to decrease its SOD and peroxidase activity. This is because the protonated amines of PAMAM in acidic solutions preadsorb OH^- on a metal surface, which helps to oxidize H_2O_2 and produce O_2 [52]. In the case of cetyltrimethylammonium bromide (CTAB) coated GNZs, cys and glutathione with carboxylic modifications enhance the peroxidase activity of GNZs towards TMB. While cys has zwitterionic interaction which further decreases the steric hindrance and increases the peroxidase activity, glutathione has spatial hindrance that leads to less enhancement of the peroxidase activity than cys [35]. A procedure was used to synthesize GNZs with peroxidase activity using reducing agents such as catechol, hydroquinone, resorcinol, vitamin C, pyrogallic acid, sodium citrate, sodium malate, and sodium tartrate. These reducing agents modify the surface of GNZs with negatively charged functional groups. The K_M value of these GNZs with a concentration of 0.1 mg/mL, was calculated towards each of H_2O_2 or TMB substrates. These GNZs with abovementioned modifications have K_M value of 0.2489, 0.4971, 0.782, 0.2258 0.8490, 1.634, 2.752, and 2.382 mg/mL towards H_2O_2, respectively. While K_M values towards TMB as substrate for these GNZs were reported to be 0.0074, 0.0153, 0.0105, 0.003, 0.0059, 0.0026, 0.0008, and 0.0016 mg/mL, respectively. Maximal reaction rate (V_{max}) of GNZs towards TMB in respect to concentration of GNZs is considered as K_{cat} and were calculated to be as 1.415, 0.464, 0.378, 0.242, 0.219, 0.084,

0.047, and 0.044 IU/mg, respectively [53]. The V_{max} and K_M values of GNZs are comparable to kinetic parameters of horseradish peroxidase (HRP) enzyme as a natural enzyme. These modifications contain different number of functional groups including hydroxyl and carboxyl, that subsequently affect the kinetic parameters of the resulted GNZs. The hydroxyl group plays the role of electron donor and the number of hydroxyl groups determines the electron density distribution. On the other hand, carboxyl groups interact with amine groups of TMB helping in adsorption of TMB as the substrate on the GNZs' surface. In enzymatic activity base biosensors, sensitivity has proportional relation with $K_M.V_{max}$ [54] and LOD has proportional relation with K_{cat}/K_M, where K_{cat}/K_M is considered as catalytic efficiency [55].

Another form of enhancement is based on synergistic effect between GNZs and a second compound, as an example Au^{III} interacts with the nitrogen atom located in a *N*-heterocyclic ligand, such as benzene and pyridine to form a complex with a catalytic activity. This activity is characterized by the electrostatic interaction and occurs when the nitrogen atom donates a σ-electron to gold and weakly accepting a π-electron [56]. To enhance the GNZs peroxidase activity towards TMB, tyrosine was used to functionalize the GNZs. Since GNZs make coordinate bonding with nitrogen atom in oxidized tyrosine, they achieve 3-fold higher peroxidase activity towards TMB substrate rather than H_2O_2 that indicates improved substrate selectivity [57]. Coupling GNZs with Prussian blue (PB) enhances the catalytic activity via the synergistic effect of GNZs and PB. Since PB has semiconductive properties, GNZs can excite an electron from the valence to the conductive band of PB, enhancing the peroxidase like activity towards TMB. In this case, GNZs-PB was assembled in a core-shell structure and H_2O_2 was detected

electrochemically using an amperometry method without applying any potential as a proof of synergistic action, see Fig. 3(d) [58]. PVP can be used to stabilize GNRs (GNZs in a nanorod shape), this modification can then be remodified with zeolite imidazolate framework-8 shell, which is assembled with Zn^{II} and 2-methylimidazolate and has a pore size of 1–2 nm. The PVP is important here because the C═O bond in PVP helps for better absorption of Zn^{II}. This combination has synergistic effect in oxidizing two neurotransmitters of serotonin and dopamine, because it has larger adsorption site and higher sensitivity. A previous study [59] used the GNR-PVP zeolite combination for the detection process of serotonin and dopamine. The results were reported in comparison with the combination of GNZs-multiwall carbon nanotube (GNZs-MWCNT). In their study, the electrochemical cyclic voltammetry was used, where in the case of the GNR-PVP-zeolite combination, the limit of detection was found to be increased by 5 times for the serotonin and 7 times for dopamine. A wide linear range as 0.1–25 μM for serotonin and 0.1–50 μM for dopamine was observed [59].

To increase the catalytic activity only towards one of the substrates, GNZs must be modified with opposite charge to that of the substrate. Unmodified GNZs show peroxidase-like activity towards both TMB and ABTS (2,2′-azino-bis(3-ethylbenzothiazoline-6-sulfonic acid)) diammonium salt [60]. Peroxidase-like activity of GNZs towards positively charged TMB is enhanced when the GNZs are modified with negatively charged organic compounds such as arabic gum, polyvinylpyrrolidone, or citrate. This catalytic activity of GNZs towards negatively charged ABTS is enhanced, where cysa is used for the modification process that causes a negatively charged surface.

Some examples show target analyte competes with the substrate on the surface of GNZs, leading to a decreased catalytic activity as a response in presence of target analyte where substrate has a role in producing a response signal for detection. Nitrite detection is important in food industry since its reaction with amine produces carcinogenic *N*-nitrosamines. To detect nitrite, the GNCs are modified with histidine since it has peroxidase activity towards TMB and nitrite. In this case, nitrite competes with TMB to be adsorbed on the active sites of the modified GNCs, where increasing the nitrite concentration inhibits the peroxidase activity towards TMB [15]. As another example, GNZs with silica modification have peroxidase activity towards TMB and a stability up to 90 days without any significant changes. However after introducing the dopamine as a neurotransmitter to the measurement solution, the GNZs starts peroxidase activity towards the dopamine because of the electroactive nature of dopamine towards H_2O_2, which helps in consuming the H_2O_2 and fading the blue color of oxidized TMB [61]. In case of cys modified GNCs due to the positive surface charge, ssDNA cannot be adsorbed on the surface of this modification. In the presence of white LED light (30 mW, 30 min), this modification is found to have oxidase activity towards TMB. Thus, when miRNA-155 is used to hybridize with ssDNA, the negatively charged phosphate backbone is exposed and electrostatically adsorbed on the surface of the GNCs-cys modification. The adsorption of the miRNA-155 hybridized ssDNA decreases the catalytic activity towards TMB and is used to detect miRNA-155 concentration [44].

3.2. Reversible catalytic activity inhibitor (RCAI)

Since GNZ act as active site, modifying its surface with some elements or molecules, or ligands makes covalent or electrostatic bonding with the surface of nanozyme and inhibit the catalytic activity of GNZs by passivating its active surface. These modification can be reversible, meaning they recover their catalytic activity in the presence of target analyte [15]. Carboxylic ligands and amine ligands decrease and increase the peroxidase activity of GNZs towards TMB, respectively. Meanwhile each of this ligands has ability to replace the other ligand on the surface of GNZs and can be used as biosensing technique to detect the other ligand [62]. Sulphides and halides make an ionic compound with Au atoms, which is stronger and relatively irreversible in compared to other modifications and can be detected while they decrease the catalytic

activity of GNZs [63]. For example, heme is a complex of iron and porphyrin, which has intrinsic peroxidase activity. When GNZs are modified with heme, a coordination bonding from the carboxylic group and metals is created. This modification (GNZs-heme) has oxidase-like catalytic activity characteristics towards TMB because of converting the valance state from Fe^{III} to Fe^{II}. Also, since GNZs-heme hybrid has oxidase-like activity, it is helpful to use heme for the detecting the presence of cys in blood. Because the cys makes thiol bonding with the GNZs, the GNZs-cys bonding is stronger than the GNZs-heme bonding. As a result of this, the cys can replace the heme causing a noticeable decrease in the oxidase activity, and consequently the cys can be detected in the blood (Fig. 3(e)) [64]. The modification of GNZs with adenosine monophosphate, adenosine diphosphate and adenosine triphosphate have peroxidase activity towards TMB. Glutathione detection is possible in this case, as it reacts with GNZs by breaking the modification, creates a stronger thiol bond on GNZs' surface and deters the peroxidase activity [65]. GNCs capped with adenosine 5-monophosphate have peroxidase like activity. GNCs entrapment in a sodium alginate (SA) hydrogel structure cross linked by Zn^{2+} as a bivalent ion, makes an egg-box structure. This structure can detect PO_4^{3-} ion concentration with a RCAI sensing strategy, because the presence of free PO_4^{3-} ions, interacts with the alginates and decompose the hydrogel structure releasing the GNCs from the egg-box structure. For example, phosphate in PBS buffer with 1 mM concentration can be detected within 3 h while it restores GNCs catalytic activity up to 93%, as seen in Fig. 4(a). The results prove that a modified GNCs with a mass ratio of SA to GNCs of 20, has high stability with the least GNCs leakage for 15 days in a pH of 7 in HEPES buffer. Measuring the catalytic activity for modified GNCs with a mass ratio of SA to GNCs of 0.5 shows 85% maintaining stability after two cycles of 300 s and has high stability for 3 days while sustaining the initial catalytic activity [66].

GNZs conjugation with aptamers specific to a type target analyte (TSAp) is a method used to increase the selectivity of sensing towards target analytes [67]. Aptamer with ssDNA or ssRNA structure can make electrostatic interaction or hydrogen bonding with the surface of modified GNZs and reversibly passivate the catalytic activity GNZs towards the substrate. Upon binding to target analyte, the TSAp leaves the surface of GNZs and restore the catalytic activity towards the substrate. The reactivation of the catalytic activity has proportional relation with their concentration [57]. This sensing platform can selectively detect a wide range of target analytes like viruses, bacteria, genome biomarkers, toxins, and other molecules [68]. As an example, acetamiprid (an agricultural pesticide) was sensed using tyrosine modified GNZs. The acetamiprid specific aptamer was denatured and snap chilled and applied to be modified on the surface of GNZs-tyrosine [69]. Glucose oxidase activity of GNZs is used to detect hsa-let-7c miRNA. In this procedure, a ssDNA complementary to hsa-let-7c miRNA type is used to as TSAp to cover the GNZs surface. The target (hsa-let-7c) is a part of miRNAs family that is associated to tumors, and it was possible to sensitively detect it, since it exhibits higher color intensity than all other miRNAs during the experiment [70]. To increase the stability of GNZs in saline environment, the bis(*p*-sulfonatophenyl)phenylphosphane dihydrate dipotassium salt (BSPP) is used as a capping agent likewise it passivates the glucose oxidase activity of GNZs. However, immobilizing a thiolated guanine rich DNA on GNZs-BSPP recovers its oxidase activity and can be used to reversibly regulate the catalytic activity on the surface of GNZs (see Fig. 4(b)). Another example used DNA modification flexible single strand structure, and the presence of K^+ ions make a conformational change producing a compact G-quadruplex shape and blocks the active site of GNZs [71]. Citrate modified GNZs also exhibits peroxidase activity towards amplex red, where oxidation product is a fluorogenic resorufin. In this reaction, the surface of GNZs is reacted and deposited with Bi^{III} elements increasing the sensitivity by 1100 times [72]. This creates a GNZs-Bi modification, which in turn can be modified with fibrinogen to detect thrombin in plasma samples. In this situation, thrombin converts
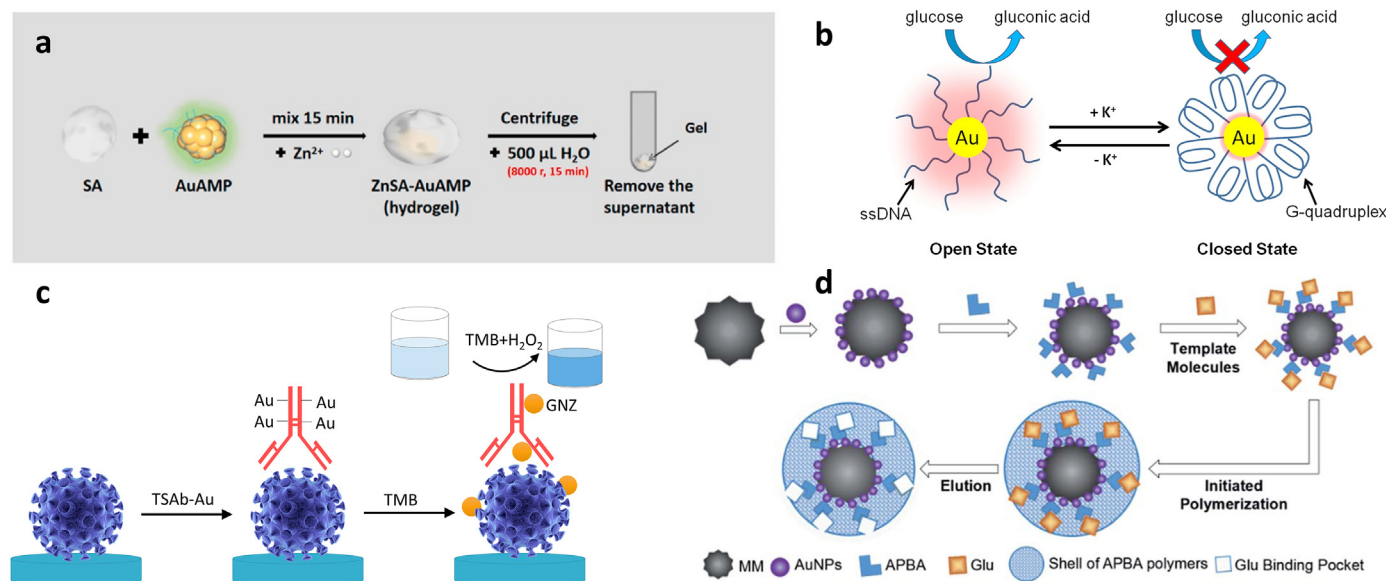
Fig. 4. Schematics using the mechanism of RCAI biosensing in the: (a) sodium alginate modified GNCs and illustration of process of releasing the GNCs in presence of phosphate, reproduced from Ref. [66] with permission from the Elsevier, copyright (2021), and (b) glucose oxidase activity of the GNZs-G-quadruplex modification, reproduced from Ref. [71], with permission from the Nature Portfolio, copyright (2015). Schematics using the mechanism of BSE biosensing in the (c) for the detection of influenza virus, redrew from Ref. [77] with permission from the Ivyspring International, copyright (2017), and (d) modification procedure of a GNZs-Pt alloy for MIP base biosensor, reproduced from Ref. [79], with permission from The Royal Society of Chemistry, copyright (2019).

fibrinogen to an insoluble fibrin form, which leads to cover the active site of GNZs and decrease the peroxidase activity. Because fibrin passivates part of the GNZs active sites, the un-passivated active sites can still react with the amplex red substrate. This type of inhibitions is referred as a mixed inhibition mechanism [73].

GNZs modified with Pd nanoparticles can lead to the cleavage of allylcarbamate in nonfluorescent pro-rhodamine 110 and produces a fluorescent product. This fluorescent dye is considered as a drug that can be used for therapeutic and fluorescence diagnosis means. To this end, a RCAI modification strategy called biorthogonal is used. In this modification, a ligand with dimethylbenzylammonium as the head is stabilized on the surface of GNZs, that can interact with the cucurbit [7]uril (CB [7]) as a gate keeper. The existence of CB [7] on the surface of GNZs creates a hindrance to inhibit any access of the non-fluorescent pro--rhodamine 110 substrate to the GNZs [74]. These modified GNZs possess enzyme-like behavior since they have catalytic activity similar to active site of nanozymes and can regulate their catalytic activity in presence of 1-adamantylamine. The 1-adamantylamine is a competing molecule to dimethylbenzylammonium [75]. It can interact with CB [7] and release it from the dimethylbenzylammonium head, recovering the catalytic activity on the surface of GNZs [74].

3.3. Binding selectivity enhancer (BSE)

Antibodies have protein domains which are binding sites with a shape complementary to a target analyte. Conjugation of antibody on GNZs is an approach to address the selectivity inefficiency of GNZs in biosensors and bioassays [76]. A nanonzyme-linked immunosorbent assay (NLISA) was implemented to detect influenza A (H5N1) as a target analyte using GNZs and TSAb (target specific antibody) conjugate. GNZs-TSAb had peroxidase activity towards TMB and high selectivity towards target analyte. As presented in Fig. 4(c), Au^{III} in the chloride salt in aqueous solution is electrostatically interacted with TSAb making an Au^{III}-TSAb mixture. The GNZs-TSAb was synthesized from the mixture, with the addition of TMB as a reducing agent. Influenza virus was adsorbed on wells of immune 96-well plate assay and was quantified based on its interaction with GNZs-TSAb and generation of amplified colorimetric response due to the peroxidase activity of GNZs-TSAb after the second addition of TMB with H_2O_2 as substrates [77].

Molecularly imprinted polymer (MIP) is a promising approach that can be used in the development of biosensors and bioassays known as synthetic antibodies. This technology causes high sensitivity, high selectivity, and a special molecular memory. MIPs can be synthesized with specific capacity of molecular recognition by introducing recognition properties into synthetic polymers. To prepare MIPs, covalent, noncovalent and sacrificial spacer methods are used to polymerize template molecules with cross-linkers and functional monomers. When the template molecule is removed from the polymer, the target molecules are recognized and adsorbed to the cavities network left behind the removed template molecules (which have the same size, shape, and chemical function selective to the template) [78]. As an example, the GNZs-Pt alloy (with Au:Pt molar ratio of 1:1) was used in preparing of MIPs. Preparation of MIPs included the use of the aminophenylboronic acid (APBA) as the polymer, and the glucose as the template molecules. In the production procedure, the GNZs-Pts are stabilized on the surface of magnetic microspheres. The APBA was then adsorbed on the GNZs-Pt surface through the electrostatic adsorption and the bonds between the nitrogen in the amine group of APBA and gold. The hydroxyl groups in glucose were then interacted with the GNZs-Pt-APBA modification under the oxygen free condition. In the presence of *N,N'*-methylenebisacrylamide (MBA) as crosslinker, a network structure of APBA was formed as a shell containing the resulted structure. Afterward, to create the MIP cavities, acidic phosphate buffer (pH = 5) was used to elute the glucose molecules, as demonstrated in Fig. 4(d). In this case, constructing a glucose selective MIP based biosensor was a successful process with 200 fold higher sensitivity than biosensor based on bare GNZs [79]. In another example the sulfadiazine antibiotic (SDZ) was detected in spiked milk and honey media using MIP with antibody mimetic characteristic. The used MIP was prepared using template molecules of SDZ, functional monomers of methacrylic acid, and cross-linkers of EGDMA (ethylene glycol dimethacrylate). Pt–SiO₂ modified GNZs were immobilized in this molecular imprinting. The modified GNZs are more inclined towards adsorbing target molecules and can detect the SDZ with a LOD value of 0.09 mg/L while 50% of catalytic activity was inhibited at 6.1 mg/L concentration of SDZ. when is The colorimetry detection method was used based on inhibiting the GNZs' nanonzymatic activity [80].

To enhance the selectivity of biosensor, aptamer is another type of bioreceptor with high affinity towards a special target analyte. As an example, GNZs with reductase-like activity towards *p*-nitrophenol was immobilized with cocaine specific aptamers. In presence of cocaine, aptamers interact with cocaine and make a junction which inhibit the entrance of *p*-aminophenol to the surface of GNZs and decrease their catalytic activity and prevent the generation of yellow colored *p*-aminophenol [81].

3.4. Agglomeration base (AB)

Some modifications of GNZs in presence of target analyte tend to lose their colloidal stability which affect the catalytic activity. This can indirectly increase or decrease the catalytic activity based on interaction between the modification and target analyte [20]. Spermine, is a polyamine with positive charge which exists in eukaryotic cells and stabilizes the structure of chromatin. Its increase in urine is a marker of cancer. One study showed that when the GNZs-Pt alloy are modified by citrate and covered by ssDNA, they show catalase activity, which can help in the detection of spermine. Addition of spermine, leads to the aggregation of GNZs by shielding the negatively charged DNA. This can block the surface that decreases the alloy's catalytic activity resulting in a change in color from red to blue and producing less O_2 gas. In this study, they used gas pressure method for the detection of spermidine within the concentration range of 0.01–1.6 μM with a LOD value of 9.6 nM. In addition to the gas pressure detection, the UV–Vis absorption was used for the detection over a range of 0.08–0.6 μM with obtained LOD of 16.8 nM that was based on the change in plasmon resonance of GNZs. This modification also causes a good selectivity towards spermine in the presence of other interfering polyamines such as spermidine, putrescine, cadaverine, phenethylamine, tyramine, tryptamine, histamine, and arginine even in 10 times higher concentration. In this study, the used interfering polyamines were [82].

In another study, GNCs with the size of 1.8 nm and a positive zeta potential (ζ) were synthesized using H[AuCl$_4$] and papain as a reducing and capping agent in 1:5 M ratio. Thus prepared GNCs showed peroxidase activity towards the TMB substrate with K_M equal to HRP enzyme, see Fig. 5(a). The UV–Vis spectroscopy was carried out to detect the absorbance of TMB oxide. Moreover, introducing dopamine with positive charge to the solution could decrease the surface charge of GNCs that resulted in aggregation and consequently their size increased up to 4.4 nm. This helps to increase the rate of catalytic activity and release of Au^I from the surface of nanozymes, resulting in enhanced oxidation of TMB and subsequently the detection of the dopamine with LOD value of 0.8 μM [83].

3.5. Multienzyme like activities (MEAs)

GNZs show various MEAs at the same time or convert their catalytic activities using rational modification techniques. These modifications for MEAs in biosensing strategy can be categorized as CS or LG, respectively [9].

3.5.1. Cascade system (CS)

In a CS the modifications with functional groups on the GNZs can be applied to grant the MEAs where a product of one enzymatic activity is the substrate for the second enzymatic activity [84]. In a GNCs-GNZs composite, when the GNZs possess glucose oxidase-like activity, the modification of the GNCs with bovine serum albumin (BSA) provides peroxidase activity towards TMB. The construction of this CS is used for detection of glucose by the colorimetry method with an LOD value of 10 μM and a linear dynamic range of 30–5000 μM [85]. Another example was when gallnut extract consists of pyrogallol and tannic acid as polyphenolic compounds was used as a reducing agent to synthesize and stabilize the GNZs by providing a ζ-potential equals to −32.2 mV. They adsorb hydroxyl groups on the surface via transferring electrons from the conductive band of GNZs. This modification provides the GNZs with peroxidase activity towards TMB which is demonstrated in Fig. 5(b). Moreover, they impart with glucose oxidase activity at the same time. The Michaelis-Menten constant K_M for H_2O_2 is 0.089 mM and for glucose
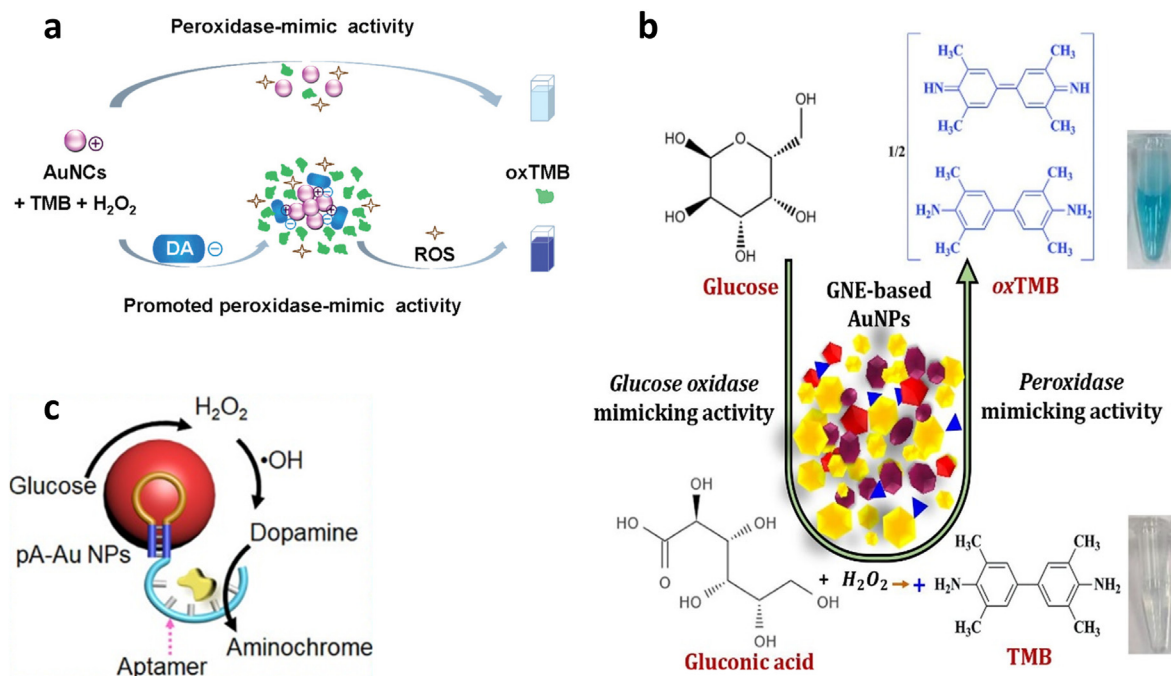

Fig. 5. Schematic diagram for the agglomeration base sensing mechanism: (a) based on agglomeration effect on peroxidase-mimic activity of GNCs towards TMB when modified with papain, reproduced from Ref. [83] with permission from The Royal Society of Chemistry, copyright (2021). Schematic diagrams for the cascade system: (b) for gallnut modified GNZs with TMB peroxidase and glucose oxidase activity, reproduced from Ref. [32] with permission from the Elsevier, copyright (2020), (c) for GNZs modified with dopamine specific aptamer for detection of dopamine, reproduced from Ref. [87] with permission from American Chemical Society, copyright (2022), and.

is 0.118 mM, which is less than citrate capped GNZs. The linear range of detection was found to be 0.05–10 mM with a limit of detection of 1.5 mM [32]. Another cascade system was for GNZs with size range of 13–50 nm, as GNZs-citrate modification possess glucose oxidase activity on its surface [38]. The oxidase activity leads to produce gluconic acid and H_2O_2 as side products. This activity will be stable because the gluconic acid blocks the surface of the GNZs preventing further catalytic reactions. Another factor to limit the glucose oxidase mechanism is to add $H[AuCl_4]$ salt, which is a precursor for increasing the size of GNZs in the presence of H_2O_2, which also leads to reduce the catalytic activity [86]. GNZs modified with citrate and conjugated with dopamine specific aptamer were used as CS. These GNZs had cascade mechanism where possessing the oxidase activity toward glucose produces gluconic acid and H_2O_2 that enables H_2O_2-mediated oxidation of dopamine because of the intrinsic peroxidase activity toward dopamine. These activities enables the oxidation of dopamine to aminochrome through the aerobic oxidation of glucose as shown in Fig. 5(c) [87].

3.5.2. Logic gate (LG)

When modifying the GNZs with two types of ions, the enzymatic activities that will appear depends on the adsorbed ion on the surface of GNZs. The appearance of the enzymatic activity is similar to the behavior of the digital logic gates (such as AND, OR, and XOR), since the detection results have different types of enzymatic activities for each used ion, which leads to the appearance of conditional results that can be described by binary numbers [88]. These logic gate biosensors behave in an array fashion and can be used in multiplex detection of target analytes [89]. GNZs with different catalytic activities can also be used in these array biosensors, as an example which is represented in Fig. 6(a), a 25-atom GNCs have gluthathione peroxidase activity while its substitution with one Cu atom or one Cd atom converts its peroxidase activity to catalase or SOD activity, respectively [90].

For example, GNZs with negatively charged citrate modification can be used in logic gate applications by depositing aurophilic ions on the surface such as Hg, Bi, Pt, and Ag. In this system, catalase activity appears if one or both of the 4700/4600 Hg^{II}/Bi^{III} atoms/ions appear on the surface of GNZs (OR gate behavior). In the case of 4800/1900 Hg^{II}/Pt^{IV} atoms/ions on the surface of GNZs, the oxidase activity appears when both ions are deposited together, because the metalophoric interaction can increase the ζ-potential of GNZs, which leads to agglomeration (AND gate behavior). The peroxidase activity is inhibited when the Ag^{I}/Bi^{III} species are deposited simultaneously, but it is boosted when one of them is deposited (XOR gate behavior) [72]. A INHIBIT-OR logic gate was designed for simultaneous detection of human immunodeficiency virus (HIV) and hepatitis C virus (HCV) genes. Pt alloyed GNZs were modified with aptamer complementary to either HIV or HCV genes. These two
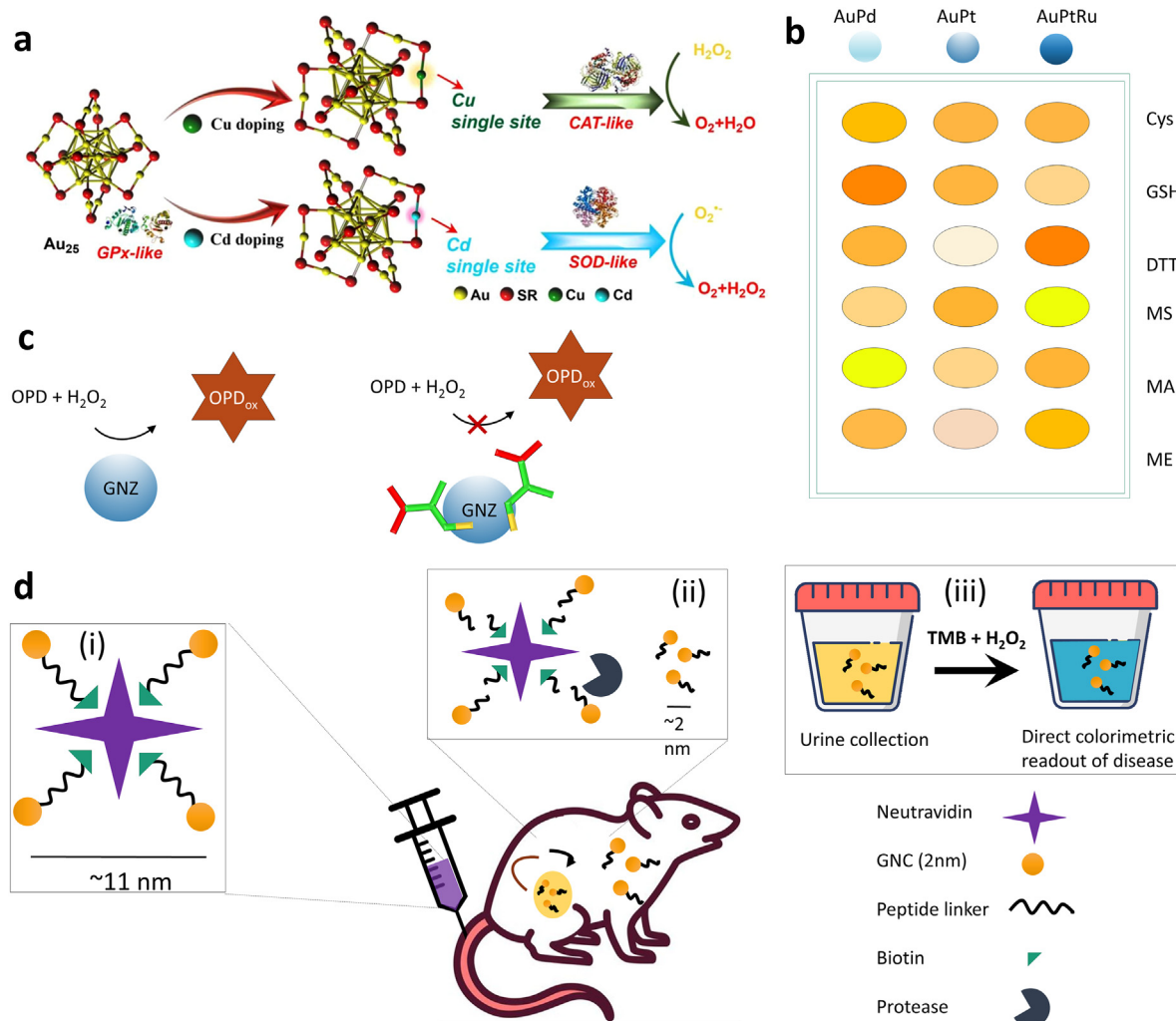
Fig. 6. Schematics of the: (a) GNCs with multienzyme like activity, reproduced from Ref. [90], Springer Nature, copyright (2021), (b) a logic gate biosensing system using three types of alloyed GNZs in array sensing, and (c) mechanism of decreased catalytic activity towards OPD in presence of cys as target analyte, reproduced from Ref. [92], with permission from The Royal Society of Chemistry, copyright (2020), and (d) *in vivo* protease biosensor using peptide modified GNCs, based on GNCs' size dependent renal clearance, redrew from Ref. [93], Springer Nature, copyright (2019).

kinds of TSAp-GNZs at the same buffer solution interact with HIV and HCV genes. Using magnetic nanoparticle modified with aptamers complementary to HIV and HCV genes the GNZs were collected from solution. The separated GNZs have peroxidase activity toward amplex red which produce a fluorescence product presenting a detectable signal for diagnosis of overall concentration of these gens. By using a masking agent specific to one type of TSAp-GNZs, catalytic activity of these TSAp-GNZs was suppressed and in this way the concentration of each type of gene was detected, where the LOD was 5 pM and linear range of detection was 10–500 pM for HIV or HCV genes concentration [91].

As demonstrated in Fig. 6(b and c) three types of GNZs alloyed with Pt, Pd, and PtRu were used in an array biosensor for detection of six types of biothiols namely glutathione, cys, mercaptoacetic acid, mercaptoethanol, mercaptosuccinic acid, dithiothreitol. Each of these alloyed GNZs had peoxidase acitivity towards OPD, that was inhibited upon the presence of a specific biothiol. Therefore, the multiplex detection of biothiols was enabled by the logical interpretation of the responses of the GNZs alloys obtained in presence of the biothiols. This method can differentiate these six types of biothiols each within the range of 1–50 μM [92].

4. Surface modification of GNZs for *in vivo* biosensing mechanisms

Surface modifications strategy of GNZs for *in vitro* sensing can be applied for *in vivo* applications, by implementing a further *in vivo* detection strategy. For example, small-sized GNCs modified with glutathione where synthesized ($\leq$5 nM) with peroxidase activity and were used with further peptide and neutravidine modifications for analysis of protease activity with *in vivo* renal clearance strategy. As shown in Fig. 6(d) by modification with a biotinated peptide on the surface, GNCs could be attached to the neutravidin a bulky protein reaching a size of 12 nm. Two types of peptides were used for modification of GNCs that were specifically cleaved in presence of matrix metalloproteinase 9 or serine proteinase thrombin which are the biomarkers of colorectal cancer or cardiovascular disease, respectively. These biomarkers after cleaving the peptide in the GNCs-peptide-neutravidin modification decrease the size of modified GNCs to 2 nm that can be cleared through the renal system due to the size filtration mechanism of kidney. In this *in vivo* sensing platform GNCs-peptide-neutravidin complex was injected intravenously. The urine sample was collected during 1 h after injection which contained GNCs with peroxidase activity towards TMB that generates an analytical signal. The signal intensity is correlated to the protease activity that can be used for the diagnosis of the cancer. The GNCs with a concentration of 1.8 μM had a K_M value of 0.23 mM and K_{cat} value of 0.2 s^{-1} towards TMB as substrate. These values for a type of HRP was 0.43 mM, and 4000 s^{-1} where HRP was 1400,000 times less concentrated than GNCs. The *in vitro* detection procedure of TMB in 25 μL urine, using 100 nM GNCs showed a LOD of 2.7 pmol. The 1.6–2.4 mg/kg of GNCs-glutathione injection in this method could differentiate the colorectal cancer diagnosed mice from healthy control providing 13 times higher colorimetry response. GNCs-Neutravidin injected in colorectal cancer diagnosed mice and collected from urine in 1 h had a 3.2% response in respect to *in vitro* GNCs-glutathione in urine sample.

For *in vivo* biosensing and theragnostic applications, further the biocompatibility of GNZs needs to be investigated [8]. The maximal tolerated dose for non-human primates and mice is 1059 mg/kg and 530 mg/kg for GNCs-glutathione and GNCs, respectively. The biodistribution study of GNCs-Neutravidin after injection to healthy mice shows accumulation of GNCs-Neutravidin in liver observed after 1 h which increases until 24 h, however a significant decrease after 1 week and complete withdraw from all organs of heart, lung, liver, spleen, and kidney was observed after 4 weeks [93]. High biocompatibility of GNZs (1.96 nm) was observed also in an other study where GNZs are hybridized with 2-dimensional aluminum-based porphyritic metal-organic framework (Al-MOF) with a thickness of 2.8 nm. The interaction of Au atoms on the surface of GNZs with nitrogen atom prevents agglomeration possibility of

small sized GNZs. Thus prepared hybrid showed high peroxidase-like activity toward H_2O_2 with K_M value of 7.94×10^{-3} M and 0.101×10^{-3} M for H_2O_2 and TMB, respectively. The toxicity tests were carried out by injecting GNZs-Al-MOF to mice and tissue staining test of heart, liver, kidney, spleen, and lung. After 7 days of injection no toxicity was observed. A cytotoxicity test was also performed on human umbilical vein endothelial cells lines with a high concentration of 500 μg/mL of GNZs/Al-MOF, which showed no cytotoxicity [94].

5. Conclusions and future perspectives

Modifications of GNZs have shown several benefits for biosensing and bioassay applications. In summary, the oxidoreductase, helicase, and phosphatase mechanisms of catalytic activities have been reviewed where GNPs catalyze or participate in these reactions. Furthermore, the oxidoreductase mechanism has been presented with more details by providing a summary for the peroxidase, oxidase, catalase, SOD, and reductase types of this mechanism.

Afterward, different surface modifications have been studied for biosensor construction, where modification interaction with target analyte determines the mechanism of detecting. GNZs proved to have numerous types of catalytic activities, that can be used to rationally design a biosensing approach along with selection of a proper surface modification. In fact, the catalytic activities of GNZs immobilized with functional groups are improved as they function similar to the active sites of natural enzymes. The substrate selectivity indicated by K_M is provided for different NZs. The surface modifications strategies of GNZs used in biosensing and bioassays, were reviewed by providing examples of modifications related to the CAE, RCAI, BSE, AB, and MEA approaches. Several examples are provided with explaining how the consequent properties of each modification strategy on GNZs lead to the enhanced sensitivity, linear range, LOD, and the efficiency of the detection process. Overall, thanks to their biocompatibility, tuneable enzymatic activity, and a wide range of modification methods, GNZs are considered as an advanced and futuristic approach for biosensing and bioassay applications.

1 Studied biosensors based on the enzyme-like activity of GNZs, mainly employ the peroxidase activity with H_2O_2 as substrate. This substrate denatures biological elements and decreases the accuracy of detection. However, GNZs possess various enzymatic activities which can be used in biosensing and bioassays instead.

2 Application of different modifications strategies on GNZs and subsequent use in biosensing and bioassays can enhance and implement different sensing properties. Rational designing the modification of GNZs enables the designing of an effective detection method based on the specific interaction of modification layer and the target analyte.

3 The AB examples are mostly provided with response signals produced from surface plasmon resonance of NZs, however more attention is needed to pay to enzyme-like characteristic of NZs in sensing of target analyte. This can include the agglomeration of the GNZs in sensing strategy upon the interaction with the target analyte that influences the enzyme-like activity of the GNZs and consequently the analytical signal.

4 GNZs with different enzyme like activities open a new horizon for more research and future applications to implement this multienzme like activities. This strategy includes the modifications which confer several enzyme-like activities to GNZs for detection. Multienzyme-like activities can be used in multiplex detection through a proper strategy such as logic gate to address the current needs in clinical analysis such as simultaneous detection of several biomarkers to increase the specificity of the diagnosis.

5 A sensing platform where the interaction of the target analyte with GNZs results in a decrease in signal, while, the RCAI strategy that enhances the catalytic activity and results in an increase in analytical signal is recommended to differentiate the non-specific adsorption

from the target analyte. RCAI strategy can also be implemented in theragnostic, since the catalytic activity is enhanced while releasing the modification from the surface. In this approach the surface modification or the enzyme-like activity provides the therapeutic applications.

6 The *in vivo* studies with GNZs were mainly focused on the therapeutic applications using enzyme-like properties of GNZs or bioimaging applications using none-enzymatic characteristics of GNZs. Hence, revising the *in vitro* biosensing strategies needs to be carried out to extend their application to the *in vivo* biosensing to eliminate the use of expensive instrumentations for diagnosis.

Declaration of competing interest

The authors declare that they have no known competing financial interests or personal relationships that could have appeared to influence the work reported in this paper.

Data availability

The authors acquired the permission for the given data in this review.

Acknowledgement

References

[1] H. Wei, E.K. Wang, Nanomaterials with enzyme-like characteristics (nanozymes): next-generation artificial enzymes, Chem. Soc. Rev. 42 (2013) 6060–6093, https://doi.org/10.1039/c3cs35486e.

[2] B. Jiang, M.M. Liang, Advances in single-atom nanozymes research(dagger), Chin. J. Chem. 39 (2021) 174–180, https://doi.org/10.1002/cjoc.202000383.

[3] F. Manea, F.B. Houillon, L. Pasquato, P. Scrimin, Nanozymes: gold-nanoparticle-based transphosphorylation catalysts, Angew. Chem., Int. Ed. 43 (2004) 6165–6169, https://doi.org/10.1002/anie.200460649.

[4] L. Liu, H. Jiang, X.M. Wang, Functionalized gold nanomaterials as biomimetic nanozymes and biosensing actuators, Trends Anal. Chem. 143 (2021), 116376, https://doi.org/10.1016/j.trac.2021.116376.

[5] S.C. Bera, K. Sanyal, D. Senapati, P.P. Mishra, Conformational changes followed by complete unzipping of DNA double helix by charge-tuned gold nanoparticles, J. Phys. Chem. B 120 (2016) 4213–4220, https://doi.org/10.1021/acs.jpcb.6b01323.

[6] B. Das, J.L. Franco, N. Logan, P. Balasubramanian, M.I. Kim, C. Cao, Nanozymes in point-of-care diagnosis: an emerging futuristic approach for biosensing, Nano-Micro Lett. 13 (2021) 193, https://doi.org/10.1007/s40820-021-00717-0.

[7] A.M. Ashrafi, Z. Bytesnikova, J. Barek, L. Richtera, V. Adam, A critical comparison of natural enzymes and nanozymes in biosensing and bioassays, Biosens. Bioelectron. 192 (2021) 113494, https://doi.org/10.1016/j.bios.2021.113494.

[8] M. Sharifi, S.H. Hosseinali, P. Yousefvand, A. Salihi, M.S. Shelcha, F.M. Aziz, A. Jouyatalaei, A. Hasan, M. Falahati, Gold nanozyme: biosensing and therapeutic activities, Mater. Sci. Eng. C 108 (2020), 110422, https://doi.org/10.1016/j.msec.2019.110422.

[9] S. Martinez, L. Veth, B. Lainer, P. Dydio, Challenges and opportunities in multicatalysis, ACS Catal. 11 (2021) 3891–3915, https://doi.org/10.1021/acscatal.0c05725.

[10] M.L. Li, D.C. Lu, R.Y. You, H.Y. Shen, L.J. Zhu, Q.Q. Lin, Y.D. Lu, Surface-enhanced Raman scattering biosensor based on self-assembled gold nanorod arrays for rapid and sensitive detection of tyrosinase, J. Phys. Chem. C 126 (2022) 12651–12659, https://doi.org/10.1021/acs.jpcc.2c03408.

[11] P.A. Frey, A.D. Hegeman, Enzymatic Reaction Mechanisms, vol. 36, 2008, pp. 247–248. Oxford, New York.

[12] L.Z. Gao, J. Zhuang, L. Nie, J.B. Zhang, Y. Zhang, N. Gu, T.H. Wang, J. Feng, D.L. Yang, S. Perrett, X. Yan, Intrinsic peroxidase-like activity of ferromagnetic nanoparticles, Nat. Nanotechnol. 2 (2007) 577–583, https://doi.org/10.1038/nnano.2007.260.

[13] Y. Jv, B.X. Li, R. Cao, Positively-charged gold nanoparticles as peroxidiase mimic and their application in hydrogen peroxide and glucose detection, Chem. Commun. 46 (2010) 8017–8019, https://doi.org/10.1039/c0cc02698k.

[14] Y.P. Chen, Y.L. Xianyu, X.Y. Jiang, Surface modification of gold nanoparticles with small molecules for biochemical analysis, Acc. Chem. Res. 50 (2017) 310–319, https://doi.org/10.1021/acs.accounts.6b00506.

[15] L.J. Huang, D.W. Sun, H.B. Pu, Q.Y. Wei, Development of nanozymes for food quality and safety detection: principles and recent applications, Compr. Rev. Food Sci. Food Saf. 18 (2019) 1496–1513, https://doi.org/10.1111/1541-4337.12485.

[16] R.F. Zhang, X.Y. Yan, K.L. Fan, Nanozymes inspired by natural enzymes, Acc. Mater. Res. 2 (2021) 534–547, https://doi.org/10.1021/accountsmr.1c00074.

[17] I. Wheeldon, S.D. Minteer, S. Banta, S.C. Barton, P. Atanassov, M. Sigman, Substrate channelling as an approach to cascade reactions, Nat. Chem. 8 (2016) 299–309, https://doi.org/10.1038/nchem.2459.

[18] B. Chatterjee, S.J. Das, A. Anand, T.K. Sharma, Nanozymes and aptamer-based biosensing, Mater. Sci. Energy Technol. 3 (2020) 127–135, https://doi.org/10.1016/j.mset.2019.08.007.

[19] J.J.X. Wu, X.Y. Wang, Q. Wang, Z.P. Lou, S.R. Li, Y.Y. Zhu, L. Qin, H. Wei, Nanomaterials with enzyme-like characteristics (nanozymes): next-generation artificial enzymes (II), Chem. Soc. Rev. 48 (2019) 1004–1076, https://doi.org/10.1039/c8cs00457a.

[20] G. Tang, J. He, J. Liu, X. Yan, K. Fan, Nanozyme for tumor therapy: surface modification matters, Explorations 1 (2021) 75–89, https://doi.org/10.1002/EXP.20210005.

[21] R.G. Mahmudunnabi, F.Z. Farhana, N. Kashaninejad, S.H. Firoz, Y.B. Shim, M.J.A. Shiddiky, Nanozyme-based electrochemical biosensors for disease biomarker detection, Analyst 145 (2020) 4398–4420, https://doi.org/10.1039/d0an00558d.

[22] C. Della Pina, E. Falletta, M. Rossi, Update on selective oxidation using gold, Chem. Soc. Rev. 41 (2012) 350–369, https://doi.org/10.1039/c1cs15089h.

[23] V. Shcherbakov, S.A. Denisov, M. Mostafavi, A mechanistic study of gold nanoparticles catalysis of O2 reduction by ascorbate and hydroethidine, investigating reactive oxygen species reactivity, RSC Adv. 13 (2023) 8557–8563, https://doi.org/10.1039/D3RA00443K.

[24] S.L. Zhuang, L.W. Liao, M.B. Li, C.H. Yao, Y. Zhao, H.W. Dong, J. Li, H.T. Deng, L.L. Li, Z.K. Wu, The fcc structure isomerization in gold nanoclusters, Nanoscale 9 (2017) 14809–14813, https://doi.org/10.1039/c7nr05239a.

[25] X.M. Shen, W.Q. Liu, X.J. Gao, Z.H. Lu, X.C. Wu, X.F. Gao, Mechanisms of oxidase and superoxide dismutation-like activities of gold, silver, platinum, and palladium, and their alloys: a general way to the activation of molecular oxygen, J. Am. Chem. Soc. 137 (2015) 15882–15891, https://doi.org/10.1021/jacs.5b10346.

[26] D.W. Jiang, D.L. Ni, Z.T. Rosenkrans, P. Huang, X.Y. Yan, W.B. Cai, Nanozyme: new horizons for responsive biomedical applications, Chem. Soc. Rev. 48 (2019) 3683–3704, https://doi.org/10.1039/c8cs00718g.

[27] J.N. Li, W.Q. Liu, X.C. Wu, X.F. Gao, Mechanism of pH-switchable peroxidase and catalase-like activities of gold, silver, platinum and palladium, Biomaterials 48 (2015) 37–44, https://doi.org/10.1016/j.biomaterials.2015.01.012.

[28] D.C. Zhang, N. Shen, J.R. Zhang, J.M. Zhu, Y. Guo, L. Xu, A novel nanozyme based on selenopeptide-modified gold nanoparticles with a tunable glutathione peroxidase activity, RSC Adv. 10 (2020) 8685–8691, https://doi.org/10.1039/c9ra10262k.

[29] S.R. Ahmed, A.C. Chen, In situ enzymatic generation of gold nanoparticles for nanozymatic label-free detection of acid phosphatase, ACS Appl. Nano Mater. 3 (2020) 9462–9469, https://doi.org/10.1021/acsanm.0c02067.

[30] S. Navalon, R. Martin, M. Alvaro, H. Garcia, Gold on diamond nanoparticles as a highly efficient Fenton catalyst, Angew. Chem., Int. Ed. 49 (2010) 8403–8407, https://doi.org/10.1002/anie.201003216.

[31] T.T. Liu, Z.W. Li, M.H. Chen, H.J. Zhao, Z.K. Zheng, L. Cui, X.M. Zhang, Sensitive electrochemical biosensor for Uracil-DNA glycosylase detection based on self-linkable hollow Mn/Ni layered doubled hydroxides as oxidase-like nanozyme for cascade signal amplification, Biosens. Bioelectron. 194 (2021), 113607, https://doi.org/10.1016/j.bios.2021.113607.

[32] A.R. Deshmukh, H. Aloui, B.S. Kim, Novel biogenic gold nanoparticles catalyzing multienzyme cascade reaction: glucose oxidase and peroxidase mimicking activity, Chem. Eng. J. 421 (2021), 127859, https://doi.org/10.1016/j.cej.2020.127859.

[33] J. Nishigaki, T. Ishida, T. Honma, M. Haruta, Oxidation of beta-nicotinamide adenine dinucleotide (NADH) by Au cluster and nanoparticle catalysts aiming for coenzyme regeneration in enzymatic glucose oxidation, ACS Sustain. Chem. Eng. 8 (2020) 10413–10422, https://doi.org/10.1021/acssuschemeng.0c01893.

[34] M. Yaseen, M. Humayun, A. Khan, M. Usman, H. Ullah, A.A. Tahir, H. Ullah, Preparation, functionalization, modification, and applications of nanostructured gold: a critical review, Energies 14 (2021) 1278, https://doi.org/10.3390/en14051278.

[35] R. Cai, X.S. Gao, C.Q. Zhang, Z.J. Hu, Y.L. Ji, J.B. Liu, X.C. Wu, Improving peroxidase activity of gold nanorod nanozymes by dragging substrates to the catalysis sites via cysteine modification, Nanotechnology 32 (2021), 485702, https://doi.org/10.1088/1361-6528/ac1e53.

[36] W. Gao, J. He, L. Chen, X. Meng, Y. Ma, L. Cheng, K. Tu, X. Gao, C. Liu, M. Zhang, K. Fan, D.-W. Pang, X. Yan, Deciphering the catalytic mechanism of superoxide dismutase activity of carbon dot nanozyme, Nat. Commun. 14 (2023) 160, https://doi.org/10.1038/s41467-023-35828-2.

[37] C. Liu, W.B. Fan, W.X. Cheng, Y.P. Gu, Y.M. Chen, W.H. Zhou, X.F. Yu, M.H. Chen, M.R. Zhu, K.L. Fan, Q.Y. Luo, Red emissive carbon dot superoxide dismutase nanozyme for bioimaging and ameliorating acute lung injury, Adv. Funct. Mater. 33 (2023), 2213856, https://doi.org/10.1002/adfm.202213856.

[38] Y. Chong, Q. Liu, C.C. Ge, Advances in oxidase-mimicking nanozymes: classification, activity regulation and biomedical applications, Nano Today 37 (2021), 101076, https://doi.org/10.1016/j.nantod.2021.101076.

[39] D.A. Rosca, J.A. Wright, D.L. Hughes, M. Bochmann, Gold peroxide complexes and the conversion of hydroperoxides into gold hydrides by successive oxygen-transfer reactions, Nat. Commun. 4 (2013) 2167, https://doi.org/10.1038/ncomms3167.

[40] N. Stasyuk, G. Gayda, T. Kavetskyy, M. Gonchar, Nanozymes with reductase-like activities: antioxidant properties and electrochemical behavior, RSC Adv. 12 (2022) 2026–2035, https://doi.org/10.1039/d1ra08127f.

[41] P. Singh, S. Roy, A. Jaiswal, Cubic gold nanorattles with a solid octahedral core and porous shell as efficient catalyst: immobilization and kinetic analysis, J. Phys. Chem. C 121 (2017) 22914–22925, https://doi.org/10.1021/acs.jpcc.7b07748.

[42] P.X. Zhao, X.W. Feng, D.S. Huang, G.Y. Yang, D. Astruc, Basic concepts and recent advances in nitrophenol reduction by gold- and other transition metal nanoparticles, Coord. Chem. Rev. 287 (2015) 114–136, https://doi.org/10.1016/j.ccr.2015.01.002.

[43] N. Ruiz-Gutierrez, M. Rieu, J. Ouellet, J.F. Allemand, V. Croquette, H. Le Hir, Chapter Thirteen - novel approaches to study helicases using magnetic tweezers, in: Methods in Enzymology, Academic Press, 2022, pp. 359–403.

[44] Y.S. Borghei, M. Hosseini, M.R. Ganjali, Oxidase-like Catalytic activity of Cys-AuNCs upon visible light irradiation and its application for visual miRNA detection, Sensor. Actuator. B Chem. 273 (2018) 1618–1626, https://doi.org/10.1016/j.snb.2018.07.061.

[45] K.G. Cabugao, C.M. Timm, A.A. Carrell, J. Childs, T.Y.S. Lu, D.A. Pelletier, D.J. Weston, R.J. Norby, Root and rhizosphere bacterial phosphatase activity varies with tree species and soil phosphorus availability in Puerto Rico tropical forest, Front. Plant Sci. 8 (2017) 1834, https://doi.org/10.3389/fpls.2017.01834.

[46] Y. Lyu, L. Morillas-Becerril, F. Mancin, P. Scrimin, Hydrolytic cleavage of nerve agent simulants by gold nanozymes, J. Hazard Mater. 415 (2021), 125644, https://doi.org/10.1016/j.jhazmat.2021.125644.

[47] J.L.Y. Chen, C. Pezzato, P. Scrimin, L.J. Prins, Chiral nanozymes-gold nanoparticle-based transphosphorylation catalysts capable of enantiomeric discrimination, Chem. Eur J. 22 (2016) 7028–7032, https://doi.org/10.1002/chem.201600853.

[48] H. Wei, L.Z. Gao, K.L. Fan, J.W. Liu, J.Y. He, X.G. Qu, S.J. Dong, E.K. Wang, X.Y. Yan, Nanozymes, A clear definition with fuzzy edges, Nano Today 40 (2021), 101269, https://doi.org/10.1016/j.nantod.2021.101269.

[49] Y. Tao, Y.H. Lin, Z.Z. Huang, J.S. Ren, X.G. Qu, Incorporating graphene oxide and gold nanoclusters: a synergistic catalyst with surprisingly high peroxidase-like activity over a broad pH range and its application for cancer cell detection, Adv. Mater. 25 (2013) 2594–2599, https://doi.org/10.1002/adma.201204419.

[50] F. Dashtestani, H. Ghourchian, A. Najafi, Silver-gold-apoferritin nanozyme for suppressing oxidative stress during cryopreservation, Mater. Sci. Eng. C 94 (2019) 831–840, https://doi.org/10.1016/j.msec.2018.10.008.

[51] H.L. Sun, J.B. Zhang, M.J. Wang, X.G. Su, Ratiometric fluorometric and colorimetric dual-mode sensing of glucose based on gold-platinum bimetallic nanoclusters, Microchem. J. 179 (2022), 107574, https://doi.org/10.1016/j.microc.2022.107574.

[52] C.P. Liu, T.H. Wu, C.Y. Liu, K.C. Chen, Y.X. Chen, G.S. Chen, S.Y. Lin, Self-supplying O-2 through the catalase-like activity of gold nanoclusters for photodynamic therapy against hypoxic cancer cells, Small 13 (2017), 1700278, https://doi.org/10.1002/smll.201700278.

[53] M.Z. Ma, J.J. Cao, A.S. Fang, Z.H. Xu, T.Y. Zhang, F. Shi, Detection and difference analysis of the enzyme activity of colloidal gold nanoparticles with negatively charged surfaces prepared by different reducing agents, Front. Chem. 9 (2022), 812083, https://doi.org/10.3389/fchem.2021.812083.

[54] R. Swaminathan, M.C. Devi, L. Rajendran, K. Venugopal, Sensitivity and resistance of amperometric biosensors in substrate inhibition processes, J. Electroanal. Chem. 895 (2021) 115527, https://doi.org/10.1016/j.jelechem.2021.115527.

[55] D.A. Huyke, A. Ramachandran, V.I. Bashkirov, E.K. Kotseroglou, T. Kotseroglou, J.G. Santiago, Enzyme kinetics and detector sensitivity determine limits of detection of amplification-free CRISPR-cas12 and CRISPR-cas13 diagnostics, Anal. Chem. 94 (2022) 9826–9834, https://doi.org/10.1021/acs.analchem.2c01670.

[56] S. Radenkovic, M. Antic, N.D. Savic, B.D. Glisic, The nature of the Au-N bond in gold(III) complexes with aromatic nitrogen-containing heterocycles: the influence of Au(III) ions on the ligand aromaticity, New J. Chem. 41 (2017) 12407–12415, https://doi.org/10.1039/c7nj02634j.

[57] P. Weerathunge, R. Ramanathan, V.A. Torok, K. Hodgson, Y. Xu, R. Goodacre, B.K. Behera, V. Bansal, Ultrasensitive colorimetric detection of murine norovirus using NanoZyme aptasensor, Anal. Chem. 91 (2019) 3270–3276, https://doi.org/10.1021/acs.analchem.8b03300.

[58] W. Zhang, C. Wang, L.H. Guan, M.H. Peng, K. Li, Y.Q. Lin, A non-enzymatic electrochemical biosensor based on Au@PBA(Ni-Fe):MoS2 nanocubes for stable and sensitive detection of hydrogen peroxide released from living cells, J. Mat. Chem. B. 7 (2019) 7704–7712, https://doi.org/10.1039/c9tb02059d.

[59] L. Zhao, G.M. Niu, F.C. Gao, K.D. Lu, Z.W. Sun, H. Li, M. Stenzel, C. Liu, Y.Y. Jiang, Gold nanorods (AuNRs) and zeolitic imidazolate framework-8 (ZIF-8) core-shell nanostructure-based electrochemical sensor for detecting neurotransmitters, ACS Omega 6 (2021) 33149–33158, https://doi.org/10.1021/acsomega.1c05529.

[60] S. Wang, W. Chen, A.L. Liu, L. Hong, H.H. Deng, X.H. Lin, Comparison of the peroxidase-like activity of unmodified, amino-modified, and citrate-capped gold nanoparticles, ChemPhysChem 13 (2012) 1199–1204, https://doi.org/10.1002/cphc.201100906.

[61] S. Ray, R. Biswas, R. Banerjee, P. Biswas, A gold nanoparticle-intercalated mesoporous silica-based nanozyme for the selective colorimetric detection of dopamine, Nanoscale Adv. 2 (2020) 734–745, https://doi.org/10.1039/c9na00508k.

[62] J.J. Zhang, Z.T. Huang, Y.Z.Y. Xie, X.Y. Jiang, Modulating the catalytic activity of gold nanoparticles using amine-terminated ligands, Chem. Sci. 13 (2022) 1080–1087, https://doi.org/10.1039/d1sc05933e.

[63] C.P. Liu, K.C. Chen, C.F. Su, P.Y. Yu, P.W. Lee, Revealing the active site of gold nanoparticles for the peroxidase-like activity: the determination of surface accessibility, Catalysts 9 (2019) 517, https://doi.org/10.3390/catal9060517.

[64] Y. Liu, Z. Chen, Z.F. Shao, R. Guo, Single gold nanoparticle-driven heme cofactor nanozyme as an unprecedented oxidase mimetic, Chem. Commun. 57 (2021) 3399–3402, https://doi.org/10.1039/d1cc00279a.

[65] L. Liu, H. Jiang, X.M. Wang, Bivalent metal ions tethered fluorescent gold nanoparticles as a reusable peroxidase mimic nanozyme, J. Anal. Test. 3 (2019) 269–276, https://doi.org/10.1007/s41664-019-00109-9.

[66] L. Liu, H. Jiang, X.M. Wang, Alkaline phosphatase-responsive Zn2+ double-triggered nucleotide capped gold nanoclusters/alginate hydrogel with recyclable nanozyme capability, Biosens. Bioelectron. 173 (2021), 112786, https://doi.org/10.1016/j.bios.2020.112786.

[67] X.Q. Tao, X. Wang, B.W. Liu, J.W. Liu, Conjugation of antibodies and aptamers on nanozymes for developing biosensors, Biosens. Bioelectron. 168 (2020), 112537, https://doi.org/10.1016/j.bios.2020.112537.

[68] F.Y. Meng, Y.Y. Xu, W.F. Dong, Y.G. Tang, P. Miao, A PCR-free voltammetric telomerase activity assay using a substrate primer on a gold electrode and DNA-triggered capture of gold nanoparticles, Microchim. Acta 185 (2018) 398, https://doi.org/10.1007/s00604-018-2936-x.

[69] P. Weerathunge, R. Ramanathan, R. Shukla, T.K. Sharma, V. Bansal, Aptamer-Controlled reversible inhibition of gold nanozyme activity for pesticide sensing, Anal. Chem. 86 (2014) 11937–11941, https://doi.org/10.1021/ac5028726.

[70] X.X. Zheng, Q. Liu, C. Jing, Y. Li, D. Li, W.J. Luo, Y.Q. Wen, Y. He, Q. Huang, Y.T. Long, C.H. Fan, Catalytic gold nanoparticles for nanoplasmonic detection of DNA hybridization, Angew. Chem., Int. Ed. 50 (2011) 11994–11998, https://doi.org/10.1002/anie.201105121.

[71] P.P. Zhou, S.S. Jia, D. Pan, L.H. Wang, J.M. Gao, J.X. Lu, J.Y. Shi, Z.S. Tang, H.J. Liu, Reversible regulation of catalytic activity of gold nanoparticles with DNA nanomachines, Sci. Rep. 5 (2015), 14402, https://doi.org/10.1038/srep14402.

[72] C.W. Lien, Y.C. Chen, H.T. Chang, C.C. Huang, Logical regulation of the enzyme-like activity of gold nanoparticles by using heavy metal ions, Nanoscale 5 (2013) 8227–8234, https://doi.org/10.1039/c3nr01836a.

[73] J.I.A. Rashid, N.A. Yusof, J. Abdullah, U. Hashim, R. Hajian, Surface modifications to boost sensitivities of electrochemical biosensors using gold nanoparticles/silicon nanowires and response surface methodology approach, J. Mater. Sci. 51 (2016) 1083–1097, https://doi.org/10.1007/s10853-015-9438-6.

[74] G.Y. Tonga, Y.D. Jeong, B. Duncan, T. Mizuhara, R. Mout, R. Das, S.T. Kim, Y.C. Yeh, B. Yan, S. Hou, V.M. Rotello, Supramolecular regulation of bioorthogonal catalysis in cells using nanoparticle-embedded transition metal catalysts, Nat. Chem. 7 (2015) 597–603, https://doi.org/10.1038/nchem.2284.

[75] S. Fedeli, J. Im, S. Gopalakrishnan, J.L. Elia, A. Gupta, D. Kim, V.M. Rotello, Nanomaterial-based bioorthogonal nanozymes for biological applications, Chem. Soc. Rev. 50 (2021) 13467–13480, https://doi.org/10.1039/d0cs00659a.

[76] X.H. Niu, X. Cheng, X.F. Ruan, D. Du, Y.H. Lin, Review-nanozyme-based immunosensors and immunoassays: recent developments and future trends, J. Electrochem. Soc. 167 (2019), 037508, https://doi.org/10.1149/2.0082003jes.

[77] S.R. Ahmed, J.C. Corredor, É. Nagy, S. Neethirajan, Amplified visual immunosensor integrated with nanozyme for ultrasensitive detection of avian influenza virus, Nanotheranostics 1 (2017) 338–345, https://doi.org/10.7150/ntno.20758.

[78] W.J. Lian, S. Liu, J.H. Yu, X.R. Xing, J. Li, M. Cui, J.D. Huang, Electrochemical sensor based on gold nanoparticles fabricated molecularly imprinted polymer film at chitosan-platinum nanoparticles/graphene-gold nanoparticles double nanocomposites modified electrode for detection of erythromycin, Biosens. Bioelectron. 38 (2012) 163–169, https://doi.org/10.1016/j.bios.2012.05.017.

[79] L. Fan, Y.S. Tian, D.D. Lou, H.A. Wu, Y. Cui, N. Gu, Y. Zhang, Catalytic gold-platinum alloy nanoparticles and a novel glucose oxidase mimic with enhanced activity and selectivity constructed by molecular imprinting, Anal. Methods 11 (2019) 4586–4592, https://doi.org/10.1039/c9ay01308c.

[80] J.B. He, L. Zhang, L.H. Xu, F.F. Kong, Z.X. Xu, Development of nanozyme-labeled biomimetic immunoassay for determination of sulfadiazine residue in foods, Adv. Polym. Technol. 2020 (2020), 7647580, https://doi.org/10.1155/2020/7647580.

[81] K. Abnous, N.M. Danesh, M. Ramezani, S.M. Taghdisi, A.S. Emrani, A novel colorimetric aptasensor for ultrasensitive detection of cocaine based on the formation of three-way junction pockets on the surfaces of gold nanoparticles, Anal. Chim. Acta 1020 (2018) 110–115, https://doi.org/10.1016/j.aca.2018.02.066.

[82] Z.D. Liu, H.Y. Zhu, H.X. Zhao, C.Z. Huang, Highly selective colorimetric detection of spermine in biosamples on basis of the non-crosslinking aggregation of ssDNA-capped gold nanoparticles, Talanta 106 (2013) 255–260, https://doi.org/10.1016/j.talanta.2012.10.079.

[83] Q. Ma, Q. Qiao, Y.F. Liu, L. Qi, Colorimetric monitoring of serum dopamine with promotion activity of gold nanocluster-based nanozymes, Analyst 146 (2021) 6615–6620, https://doi.org/10.1039/d1an01511g.

[84] Z. Wang, Y. Zhao, Y. Hou, G. Tang, R. Zhang, Y. Yang, X. Yan, K. Fan, A thrombin-activated peptide-templated nanozyme for remedying ischemic stroke via thrombolytic and neuroprotective actions, Adv. Mater. 35 (2023), 2210144, https://doi.org/10.1002/adma.202210144.

[85] J.X. Chen, W.W. Wu, L. Huang, Q. Ma, S.J. Dong, Self-indicative gold nanozyme for H2O2 and glucose sensing, Chem. Eur J. 25 (2019) 11940–11944, https://doi.org/10.1002/chem.201902288.

[86] M. Zandieh, J.W. Liu, Nanozyme catalytic turnover and self-limited reactions, ACS Nano 15 (2021) 15645–15655, https://doi.org/10.1021/acsnano.1c07520.

[87] Y. Ouyang, M. Fadeev, P. Zhang, R. Carmieli, J. Li, Y.S. Sohn, O. Karmi, R. Nechushtai, E. Pikarsky, C.H. Fan, I. Willner, Aptamer-modified Au nanoparticles: functional nanozyme bioreactors for cascaded catalysis and catalysts for chemodynamic treatment of cancer cells, ACS Nano 16 (2022) 18232–18243, https://doi.org/10.1021/acsnano.2c05710.

[88] E.A. Barnoy, M. Motiei, C. Tzror, S. Rahimipour, R. Popovtzer, D. Fixler, Biological logic gate using gold nanoparticles and fluorescence lifetime imaging microscopy, ACS Appl. Nano Mater. 2 (2019) 6527–6536, https://doi.org/10.1021/acsanm.9b01457.

[89] Y.H. Lai, S.C. Sun, M.C. Chuang, Biosensors with built-in biomolecular logic gates for practical applications, Biosensors 4 (2014) 273–300, https://doi.org/10.3390/bios4030273.

[90] H.L. Liu, Y.H. Li, S. Sun, Q. Xin, S.H. Liu, X.Y. Mu, X. Yuan, K. Chen, H. Wang, K. Varga, W.B. Mi, J. Yang, X.D. Zhang, Catalytically potent and selective clusterzymes for modulation of neuroinflammation through single-atom substitutions, Nat. Commun. 12 (2021) 114, https://doi.org/10.1038/s41467-020-20275-0.

[91] X.D. Lin, Y.Q. Liu, Z.H. Tao, J.T. Gao, J.K. Deng, J.J. Yin, S. Wang, Nanozyme-based bio-barcode assay for high sensitive and logic-controlled specific detection of multiple DNAs, Biosens. Bioelectron. 94 (2017) 471–477, https://doi.org/10.1016/j.bios.2017.01.008.

[92] J.S. Lin, Q. Wang, X.Y. Wang, Y.Y. Zhu, X. Zhou, H. Wei, Gold alloy-based nanozyme sensor arrays for biothiol detection (vol 53, pg 964, 2020), Analyst 145 (2020), https://doi.org/10.1039/D0AN00451K, 4050-4050.

[93] C.N. Loynachan, A.P. Soleimany, J.S. Dudani, Y.Y. Lin, A. Najer, A. Bekdemir, Q. Chen, S.N. Bhatia, M.M. Stevens, Renal clearable catalytic gold nanoclusters for in vivo disease monitoring, Nat. Nanotechnol. 14 (2019) 883–890, https://doi.org/10.1038/s41565-019-0527-6.

[94] W.C. Hu, M.R. Younis, Y. Zhou, C. Wang, X.H. Xia, In situ fabrication of ultrasmall gold nanoparticles/2D MOFs hybrid as nanozyme for antibacterial therapy, Small 16 (2020), 2000553, https://doi.org/10.1002/smll.202000553.

[95] O. Smutok, T. Kavetskyy, T. Prokopiv, R. Serkiz, R. Wojnarowska-Nowak, O. Sausa, I. Novak, D. Berek, A. Melman, M. Gonchar, New micro/nanocomposite with peroxidase-like activity in construction of oxidases-based amperometric biosensors for ethanol and glucose analysis, Anal. Chim. Acta 1143 (2021) 201–209, https://doi.org/10.1016/j.aca.2020.11.052.

[96] L.Y. Zhang, C. Fan, M. Liu, F.J. Liu, S.S. Bian, S.Y. Du, S.Y. Zhu, H. Wang, Biominerized gold-Hemin@MOF composites with peroxidase-like and gold catalysis activities: a high-throughput colorimetric immunoassay for alpha-fetoprotein in blood by ELISA and gold-catalytic silver staining, Sensor. Actuator. B Chem. 266 (2018) 543–552, https://doi.org/10.1016/j.snb.2018.03.153.

[97] W. Huang, Y. Xu, Z.P. Wang, K. Liao, Y. Zhang, Y.M. Sun, Dual nanozyme based on ultrathin 2D conductive MOF nanosheets intergraded with gold nanoparticles for electrochemical biosensing of H2O2 in cancer cells, Talanta 249 (2022), 123612, https://doi.org/10.1016/j.talanta.2022.123612.

[98] L. Long, R. Cai, J.B. Liu, X.C. Wu, A novel nanoprobe based on core-shell Au@Pt@mesoporous SiO(2)Nanozyme with enhanced activity and stability for mumps virus diagnosis, Front. Chem. 8 (2020) 463, https://doi.org/10.3389/fchem.2020.00463.

[99] Y. Tao, E.G. Ju, J.S. Ren, X.G. Qu, Bifunctionalized mesoporous silica-supported gold nanoparticles: intrinsic oxidase and peroxidase catalytic activities for antibacterial applications, Adv. Mater. 27 (2015) 1097–1104, https://doi.org/10.1002/adma.201405105.

[100] X.Y. Ji, Q. Lu, X.H. Sun, L.Y. Zhao, Y.H. Zhang, J.S. Yao, X. Zhang, H. Zhao, Dual-active Au@PNIPAm nanozymes for glucose detection and intracellular H2O2 modulation, Langmuir (2022) 8077–8086, https://doi.org/10.1021/acs.langmuir.2c00911.

[101] N.R. Nirala, R. Prakash, Vinita, One step synthesis of AuNPs@MoS2-QDs composite as a robust peroxidase- mimetic for instant unaided eye detection of glucose inserum, saliva and tear, Sensor. Actuator. B Chem. 263 (2018) 109–119, https://doi.org/10.1016/j.snb.2018.02.085.

[102] X.L. Zhu, X.X. Mao, Z.H. Wang, C. Feng, G.F. Chen, G.X. Li, Fabrication of nanozyme@DNA hydrogel and its application in biomedical analysis, Nano Res. 10 (2017) 959–970, https://doi.org/10.1007/s12274-016-1354-9.

[103] J. Czescik, S. Zamolo, T. Darbre, R. Rigo, C. Sissi, A. Pecina, L. Riccardi, M. De Vivo, F. Mancin, P. Scrimin, A gold nanoparticle nanonuclease relying on a Zn(II) mononuclear complex, Angew. Chem. Int. Ed. 60 (2021) 1423–1432, https://doi.org/10.1002/anie.202012513.

[104] M.X. Mao, R. Zheng, C.F. Peng, X.L. Wei, DNA-gold nanozyme-modified paper device for enhanced colorimetric detection of mercury ions, Biosensors 10 (2020) 211, https://doi.org/10.3390/bios10120211.

[105] G.H. Jin, E. Ko, M.K. Kim, V.K. Tran, S.E. Son, Y. Geng, W. Hur, G.H. Seong, Graphene oxide-gold nanozyme for highly sensitive electrochemical detection of hydrogen peroxide, Sensor. Actuator. B Chem. 274 (2018) 201–209, https://doi.org/10.1016/j.snb.2018.07.160.

[106] S.M. Sun, R. Zhao, S.M. Feng, Y.L. Xie, Colorimetric zearalenone assay based on the use of an aptamer and of gold nanoparticles with peroxidase-like activity, Microchim. Acta 185 (2018) 535, https://doi.org/10.1007/s00604-018-3078-x.

[107] H.X. Ouyang, S.M. Ling, A.H. Liang, Z.L. Jiang, A facile aptamer-regulating gold nanoplasmonic SERS detection strategy for trace lead ions, Sensor. Actuator. B Chem. 258 (2018) 739–744, https://doi.org/10.1016/j.snb.2017.12.009.

[108] R. Das, A. Dhiman, A. Kapil, V. Bansal, T.K. Sharma, Aptamer-mediated colorimetric and electrochemical detection of Pseudomonas aeruginosa utilizing peroxidase-mimic activity of gold NanoZyme, Anal. Bioanal. Chem. 411 (2019) 1229–1238, https://doi.org/10.1007/s00216-018-1555-z.

[109] C.S. Wang, C. Liu, J.B. Luo, Y.P. Tian, N.D. Zhou, Direct electrochemical detection of kanamycin based on peroxidase-like activity of gold nanoparticles, Anal. Chim. Acta 936 (2016) 75–82, https://doi.org/10.1016/j.aca.2016.07.013.

[110] M.M. Shah, W. Ren, J. Irudayaraj, A.A. Sajini, M.I. Ali, B. Ahmad, Colorimetric detection of organophosphate pesticides based on acetylcholinesterase and cysteamine capped gold nanoparticles as nanozyme, Sensors 21 (2021) 8050, https://doi.org/10.3390/s21238050.

[111] S. Bhagat, N.V.S. Vallabani, V. Shutthanandan, M. Bowden, A.S. Karakoti, S. Singh, Gold core/ceria shell-based redox active nanozyme mimicking the biological multienzyme complex phenomenon, J. Colloid Interface Sci. 513 (2018) 831–842, https://doi.org/10.1016/j.jcis.2017.11.064.

[112] Z.J. Zhang, X.H. Zhang, B.W. Liu, J.W. Liu, Molecular imprinting on inorganic nanozymes for hundred-fold enzyme specificity, J. Am. Chem. Soc. 139 (2017) 5412–5419, https://doi.org/10.1021/jacs.7b00601.

[113] M. Liu, H.M. Zhao, S. Chen, H.T. Yu, X. Quan, Interface engineering catalytic graphene for smart colorimetric biosensing, ACS Nano 6 (2012) 3142–3151, https://doi.org/10.1021/nn3010922.

[114] S. Kumar, P. Bhushan, S. Bhattacharya, Facile synthesis of Au@Ag-hemin decorated reduced graphene oxide sheets: a novel peroxidase mimetic for ultrasensitive colorimetric detection of hydrogen peroxide and glucose, RSC Adv. 7 (2017) 37568–37577, https://doi.org/10.1039/c7ra06973a.

[115] L. Wu, W.M. Yin, X.C. Tan, P. Wang, F. Ding, H. Zhang, B.R. Wang, W.Y. Zhang, H.Y. Han, Direct reduction of HAuCl4 for the visual detection of intracellular hydrogen peroxide based on Au-Pt/SiO2 nanospheres, Sensor. Actuator. B Chem. 248 (2017) 367–373, https://doi.org/10.1016/j.snb.2017.03.166.

[116] Y.H. Hu, H.J. Cheng, X.Z. Zhao, J.J. Wu, F. Muhammad, S.C. Lin, J. He, L.Q. Zhou, C.P. Zhang, Y. Deng, P. Wang, Z.Y. Zhou, S.M. Nie, H. Wei, Surface-enhanced Raman scattering active gold nanoparticles with enzyme-mimicking activities for measuring glucose and lactate in living tissues, ACS Nano 11 (2017) 5558–5566, https://doi.org/10.1021/acsnano.7b00905.

[117] Y. Liu, D. Ding, Y.L. Zhen, R. Guo, Amino acid-mediated 'turn-off/turn-on' nanozyme activity of gold nanoclusters for sensitive and selective detection of copper ions and histidine, Biosens. Bioelectron. 92 (2017) 140–146, https://doi.org/10.1016/j.bios.2017.01.036.

[118] Y.Q. Chang, Z. Zhang, J.H. Hao, W.S. Yang, J.L. Tang, BSA-stabilized Au clusters as peroxidase mimetic for colorimetric detection of Ag+, Sensor. Actuator. B Chem. 232 (2016) 692–697, https://doi.org/10.1016/j.snb.2016.04.039.

[119] Y.L. Liu, W.L. Fu, C.M. Li, C.Z. Huang, Y.F. Li, Gold nanoparticles immobilized on metal-organic frameworks with enhanced catalytic performance for DNA detection, Anal. Chim. Acta 861 (2015) 55–61, https://doi.org/10.1016/j.aca.2014.12.032.

[120] M.S. Hizir, M. Top, M. Balcioglu, M. Rana, N.M. Robertson, F.S. Shen, J. Sheng, M.V. Yigit, Multiplexed activity of perAuxidase: DNA-capped AuNPs act as adjustable peroxidase, Anal. Chem. 88 (2016) 600–605, https://doi.org/10.1021/acs.analchem.5b03926.

[121] J.E. Yang, Y.X. Lu, L. Ao, F.Y. Wang, W.J. Jing, S.C. Zhang, Y.Y. Liu, Colorimetric sensor array for proteins discrimination based on the tunable peroxidase-like activity of AuNPs-DNA conjugates, Sensor. Actuator. B Chem. 245 (2017) 66–73, https://doi.org/10.1016/j.snb.2017.01.119.

[122] J.T. Hu, P.J. Ni, H.C. Dai, Y.J. Sun, Y.L. Wang, S. Jiang, Z. Li, Aptamer-based colorimetric biosensing of abrin using catalytic gold nanoparticles, Analyst 140 (2015) 3581–3586, https://doi.org/10.1039/c5an00107b.

[123] J.P. Tian, Aptamer-based colorimetric detection of various targets based on catalytic Au NPs/Graphene nanohybrids, Sens. BioSens. Res. 22 (2019), 100258, https://doi.org/10.1016/j.sbsr.2019.100258.

[124] L. Gao, M.Q. Liu, G.F. Ma, Y.L. Wang, L.N. Zhao, Q. Yuan, F.P. Gao, R. Liu, J. Zhai, Z.F. Chai, Y.L. Zhao, X.Y. Gao, Peptide-conjugated gold nanoprobe: intrinsic nanozyme-linked immunsorbant assay of integrin expression level on cell membrane, ACS Nano 9 (2015) 10979–10990, https://doi.org/10.1021/acsnano.5b04261.

[125] M.K. Masud, S. Yadav, M.N. Isam, N.T. Nguyen, C. Salomon, R. Kline, H.R. Alamri, Z.A. Alothman, Y. Yamauchi, M.S.A. Hossain, M.J.A. Shiddiky, Gold-loaded nanoporous ferric oxide nanocubes with peroxidase-mimicking activity for electrocatalytic and colorimetric detection of autoantibody, Anal. Chem. 89 (2017) 11005–11013, https://doi.org/10.1021/acs.analchem.7b02880.

[126] L.Z. Hu, D. Ding, L.Y. Feng, M. Wang, W.S. Fu, Accelerating the peroxidase-like activity of gold nanoclusters at neutral pH for colorimetric detection of heparin and heparinase activity, Anal. Chem. 90 (2018) 6247–6252, https://doi.org/10.1021/acs.analchem.8b00885.

[127] J. Liu, W. Zhang, H.L. Zhang, Z.Y. Yang, T.R. Li, B.D. Wang, X. Huo, R. Wang, H.T. Chen, A multifunctional nanoprobe based on Au-Fe3O4 nanoparticles for multimodal and ultrasensitive detection of cancer cells, Chem. Commun. 49 (2013) 4938–4940, https://doi.org/10.1039/c3cc41984c.

[128] S.K. Maji, A.K. Mandal, K.T. Nguyen, P. Borah, Y.L. Zhao, Cancer cell detection and therapeutics using peroxidase-active nanohybrid of gold nanoparticle-loaded mesoporous silica-coated graphene, ACS Appl. Mater. Interfaces 7 (2015) 9807–9816, https://doi.org/10.1021/acsami.5b01758.

[129] Y. Tao, M.Q. Li, B. Kim, D.T. Auguste, Incorporating gold nanoclusters and target-directed liposomes as a synergistic amplified colorimetric sensor for HER2-positive breast cancer cell detection, Theranostics 7 (2017) 899–911, https://doi.org/10.7150/thno.17927.

[130] I.M. Khoris, K. Takemura, J. Lee, T. Hara, F. Abe, T. Suzuki, E.Y. Park, Enhanced colorimetric detection of norovirus using in-situ growth of Ag shell on Au NPs,

Biosens. Bioelectron. 126 (2019) 425–432, https://doi.org/10.1016/j.bios.2018.10.067.

[131] C. Zhao, C.Y. Hong, Z.Z. Lin, X.M. Chen, Z.Y. Huang, Detection of Malachite Green using a colorimetric aptasensor based on the inhibition of the peroxidase-like activity of gold nanoparticles by cetyltrimethylammonium ions, Microchim. Acta 186 (2019) 322, https://doi.org/10.1007/s00604-019-3436-3.

[132] C. Mcvey, N. Logan, N.T.K. Thanh, C. Elliott, C. Cao, Unusual switchable peroxidase-mimicking nanozyme for the determination of proteolytic biomarker, Nano Res. 12 (2019) 509–516, https://doi.org/10.1007/s12274-018-2241-3.